Realized Illiquidity*

Demetrio Lacava † Angelo Ranaldo‡ Paolo Santucci de Magistris §

March 15, 2023

Abstract

Realized illiquidity is the ratio between realized volatility and trading volume refining the popular price impact measure proposed by Amihud (2002). We provide its theoretical foundation in which both price volatility, $\sigma(t)$, and market liquidity, $\ell(t)$, follow stochastic processes in continuous time. We prove that the realized illiquidity is a precise measurement of the inverse of *integrated liquidity*, that is, the integral of $\ell(t)$ over periods of unit length (e.g., a day). A comprehensive econometric analysis highlights the main distributional and dynamic properties of the realized illiquidity, including jumps, clustering, and leverage effects, and demonstrate that they help explain the time series of stock and currency returns.

Keywords: Liquidity, Stochastic Volatility, Trading Volume, Amihud, Jumps.

J.E.L. classification: C15, F31, G12, G15

*We are grateful to Yakov Amihud, Tim Bollerslev, Nicola Borri, Massimiliano Caporin, Alessandro Casini, Leopoldo Catania, Dobrislav Dobrev, Deniz Erdemlioglu, Mark Hallin, Joel Hasbrouck, Mark Podolskij, Anders Rahbek, Eduardo Rossi, Francesco Sangiorgi, Pierluigi Vallarino, and Paolo Vitale for their relevant comments about our work. We thank Kim Christensen for having shared with us the realized volatility series of SPY. We also thank the participants at the Vieco conference (Copenhagen University, 2022), IAAE conference (King's College, 2022), SoFiE conference (Cambridge, 2022), Rome-Waseda Time Series Symposium (Rome, 2022), and the seminar participants at University of Pavia, at Luiss University and at IESEG School of Management. Angelo Ranaldo acknowledges financial support from the Swiss National Science Foundation (SNSF grant 182303). Paolo Santucci de Magistris also acknowledges the research support of the Project 2 grant of the Danish Council for Independent Research (IRFD), Social Sciences, number 8019-00015A.

†Luiss "Guido Carli" University, Department of Economics and Finance, Viale Romania 32, 00197 Roma, Italy

‡University of St. Gallen and Swiss Finance Institute, Switzerland. angelo.ranaldo@unisg.ch

§Luiss "Guido Carli" University, Department of Economics and Finance, Viale Romania 32, 00197 Roma, Italy; Department of Economics and Business Economics, Aarhus University, Denmark. sdemagistris@luiss.it

1 Introduction

In addition to being crucial to the quality of financial markets and resilience of the financial system, market liquidity is important for capital market efficiency because "liquidity of investment markets often facilitates, though it sometimes impedes, the course of new investment" (Keynes, 1936, p.102). However, market liquidity is an elusive concept because it includes everything that determines "the degree to which an order can be executed within a short time frame at a price close to the security's consensus value" (Foucault et al., 2013, p.2). Thus, liquidity manifests itself in at least two important ways: the transaction cost and the impact of transaction volume on security prices, which, in turn, depends on the market depth and price elasticity. The transaction cost is often gauged by the bid-ask spread, while a popular measure for price impact is the Amihud illiquidity measure (Amihud, 2002), which is the ratio between the daily absolute returns and trading volume.[1]

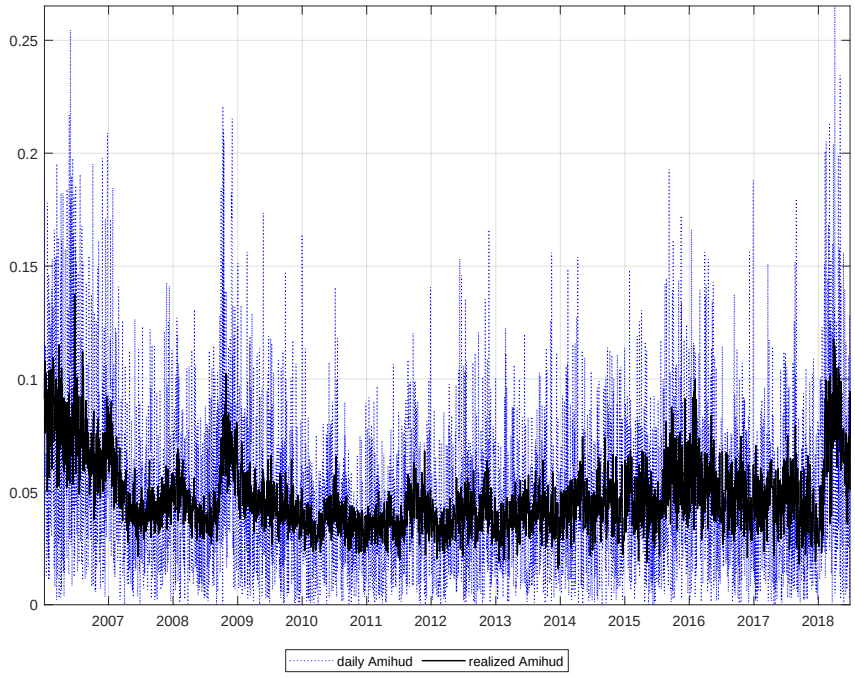

Figure 1: Realized Amihud (black solid line) vs classic daily Amihud (blue dotted line, see Amihud, 2002) of SPY. Realized Amihud is computed as the ratio between realized power variation and trading volume. Sample period: January 3, 2006 – June 29, 2018. Both series are scaled by a factor of E+09.

In this paper, we study the theoretical and empirical properties of a refinement of the classic *daily Amihud*, namely the *realized illiquidity*, which is defined as the ratio between a realized volatility measure and the daily trading volume.[2] We propose two measures of realized illiquidity that we call *realized Amihud* and *high-low Amihud*. The former is computed as the ratio between realized power variation (Barndorff-Nielsen and Shephard, 2003) using intraday data and daily trading volume.

[1] To date, the ILLIQ measure proposed by Amihud (2002) has been cited more than 11,000 times according to Google Scholar. Many of these papers were published in top-tier academic journals in finance.

[2] Although the empirical analysis focuses on the realized illiquidity computed at daily frequency, our theory and metrics can be applied to shorter (intraday) or longer (e.g., weekly or monthly) horizons.

The latter is the ratio between the daily high-low range (Parkinson, 1980) and the daily volume. Both numerators are measures of realized volatility but the former requires intraday data while the latter relies on daily data often accessible for many financial securities. Figure 1 provides a simple illustration of the precision of the realized Amihud (black solid line) in relation to the daily Amihud (blue solid line) using the SPDR S&P 500 ETF (ticker SPY) as an indication of the U.S. stock market behavior. Although both series follow similar dynamic patterns, the classic daily Amihud is much noisier than the realized Amihud.

This paper contributes to the literature in three ways. Our first contribution is outlining a simple theoretical framework based on the trading mechanism of Tauchen and Pitts (1983), which fits suitably into the theory of realized volatility, specifically here in the context of liquidity measurement. In developing the theory of realized illiquidity, we consider a setting where both spot volatility, $\sigma(t)$, and the instantaneous liquidity parameter, $\ell(t)$, are (possibly correlated) continuous-time stochastic processes. We prove that the realized illiquidity provides a measurement of the *integrated illiquidity*, which is defined as the reciprocal of $\int_0^1 \ell(s)ds$ over periods of unit length (e.g., a day, a week, or a month). This allows us to establish *how precisely* the realized illiquidity measures the integrated illiquidity vis-a-vis the classic daily Amihud, which is a special case of the realized Amihud when only one observation per period (i.e. daily return) is available. Thanks to its intrinsic non-parametric nature, the realized illiquidity represents a simple (inverse) measure of market resiliency, that is, the elasticity of asset prices to trading volume, where the latter depends on the degree of disagreement in the beliefs among traders.

A set of Monte Carlo simulations illustrates the finite sample accuracy of the realized illiquidity as a nonparametric measurement of integrated illiquidity. In the Monte Carlo simulations, we explore the finite-sample properties of the realized and high-low Amihud measures compared to the classic Amihud proxy. The numerical analysis clearly shows two results: First, the realized Amihud provides a very precise measurement of illiquidity even after considering microstructure frictions such as bid-ask spread and price discreteness. Second, although less precise than the realized Amihud, the high-low Amihud provides estimates of the underlying integrated illiquidity process that are several times more precise than those obtained by the classic daily Amihud. For these reasons, the realized Amihud can be considered the most efficient measure of realized illiquidity while the high-low Amihud is a more efficient *low*-frequency measure than the classic daily Amihud proxy.

Our second contribution is to derive a simple theory for *jumps* in illiquidity, which are generated by impactful news common to all traders such as earnings press releases for stocks or central bank announcements for currencies. The natural interpretation of such jumps is the consensual price change induced by new fundamental information for which little or no transaction volume is needed. We refer to them as *information jumps*. These events induce large volatility but little to no volume, thus increasing the observed market illiquidity due to the predominant information component. Building on the results of Barndorff-Nielsen and Shephard (2003, 2004, 2006), we develop a formal way to carry out nonparametric statistical inference on information jumps and disentangle the illiquidity generated by information jumps from the baseline illiquidity associated with disagreement among traders, which is the main driver of trading volume. In particular, we define a test statistic to detect significant jumps, and we construct the jump-robust version of the realized illiquidity estimator.

Our third contribution is to empirically study the properties of the realized illiquidity. To do so, we consider a comprehensive set of econometric specifications with the goal of characterizing the main dynamic and distributional properties of the realized Amihud. Inspired by the techniques usually adopted in the context of volatility modeling, we consider a multiplicative error model (MEM) specification (Engle and Gallo, 2006) that allows for a direct prediction of illiquidity without resorting to nonlinear transformations to preserve positivity. Furthermore, we investigate whether the slow decaying rate of the autocorrelation function of the realized Amihud is well characterized by the heterogeneous autoregressive specification (HAR) model of Corsi (2009) in both a linear and nonlinear context. All this should bring to light the predictive factors of market liquidity and evidence to support heterogeneity of trading activity of market participants operating with different investment horizons, i.e. daily, weekly, or monthly. Another well-known feature of volatility is that volatility follows asymmetric patterns with respect to positive and negative returns – that is – bad news (negative return shocks) increases volatility by more than good news (positive return shocks). We study whether a similar asymmetric mechanism characterizes illiquidity to find whether liquidity systematically evaporates more when bad news hits, as predicted by theoretical models of binding capital constraints leading to sudden liquidity dry-ups.[3] Reminiscent of two key terms used in the volatility literature, we call the first and second features *heterogeneous illiquidity clustering* and *leverage effect*, respectively.

We consider two categories of financial securities in our empirical analysis: stocks and currencies. Specifically, the time series analysis of the daily realized illiquidity of the main exchange traded fund (ETF) tracking the S&P 500 index (SPY) reveals four main findings shedding new light on the stochastic features of illiquidity. First, the empirical evidence strongly suggests that the latent illiquidity process is a very persistent one that is characterized by long periods of high illiquidity followed by long periods of low illiquidity (clustering). This persistence runs along heterogeneous horizons in that today's illiquidity is predicted not only by that of yesterday, but also by that of the previous week and month with greater intensity (heterogeneous clustering). All this suggests that there are distinct groups of traders with different behaviors, trading schedules, and time horizons, and this heterogeneity impacts the illiquidity timing with important asset pricing implications (Amihud and Mendelson, 1986).[4] Second, we find strong evidence that liquidity tends to dry up more in market downturns (leverage effect) and we demonstrate that ceteris paribus, a liquidity shock has more persistent effects when combined with negative returns. Third, when regressing excess returns on the realized Amihud, we find a significant negative coefficient. After breaking down illiquidity in its expected and unexpected components, we find that it is rather the unexpected part of illiquidity that negatively predicts returns consistent with the idea that the persistent effect of an illiquidity shock increases expected future illiquidity thus decreasing asset prices. Fourth, all these findings (i.e. heterogeneous clustering, leverage effect, and how illiquidity is associated with stock returns) are much less evident when the noisy classic daily Amihud is employed, hence reiterating the importance of using a more precise illiquidity measure.

[3] Hameed et al. (2010) provide empirical support and comprehensive discussion of this literature.

[4] In reference to this idea, previous literature has used the broad concept of Heterogeneous Market Hypothesis (Müller et al., 1993).

To conclude our empirical analysis, we examine the currency market by focusing on EUR/CHF and USD/CHF exchange rates surrounding the cap removal of the Swiss franc by the Swiss National Bank (SNB) on January 15, 2015. Despite its simplicity, our theory lends itself to several extensions that succeed in explaining and measuring illiquidity in reaction to major events such as a currency regime change. Through the lenses of our theory, the SNB announcement represents an ideal framework for testing the empirical prediction that the observed illiquidity should increase after the cap removal because the Swiss National Bank ceased to supply Swiss francs in unlimited quantities, thus reducing the supply of extra trading volume to the market. By carrying out the break analysis of Bai and Perron (1998), we find strong evidence that illiquidity significantly increased after January 15, 2015, as a joint consequence of an increase in EUR/CHF volatility and a reduction in trading volume of the same currency pair. Notably, we find an analogous pattern on the USD/CHF rate, suggesting that a liquidity shock in one market (or FX rate) immediately spills over into another one.

Our paper adds to prior research on market microstructure and liquidity. The popular Amihud (2002) measure is part of a large literature going back half a century that includes a wide range of illiquidity measures based on price changes and volume (e.g. Silber, 1975, Dubofsky and Groth, 1984). Ideally, to measure the volume price impact, one would need access to data on all orders submitted by traders in a centralized market. However, many markets are decentralized and opaque, such as all the over-the-counter (OTC) markets, including the FX market that we also study here. In this context, the classic daily Amihud measure is extremely useful for approximating the order flow impact on security prices because (a) it is an observable and non-parametric quantity and (b) it is based on daily price and volume data, much more accessible than tick-by-tick orders and transactions.[5] This is why the Amihud measure is so widely used and it has been loosely associated with the Kyle (1985) model that provides an insightful theoretical framework to explain how orders impact asset prices, as captured by his *lambda* factor.[6] Our theoretical contribution is to provide a general theory for realized illiquidity of which the Amihud measure is a specific case. Our empirical contribution is to demonstrate the superior accuracy of the realized Amihud measure, its characteristics, and explanatory power on asset returns.

Ranaldo and Santucci de Magistris (2022) adopt the realized Amihud to empirically investigate the price impact in the global FX market. We extend their work in three ways. First, we provide a theoretical foundation to the Amihud measure, which includes the notions of integrated illiquidity and jumps. Second, we study the appropriate econometric modeling that highlights the main empirical features of the realized Amihud measures, including illiquidity jumps, heterogeneous clustering, and leverage effects, and how they explain asset returns. Finally, we propose two methods, i.e. the high-low Amihud and the realized one. Both metrics share the advantages of the Amihud measure – that is – they are easy-to-compute and rely on the ratio between two observable quantities based on transaction data, namely volume and (realized) volatility (measured either as high-low range or realized power variation). In doing so, the high-low and realized measures extend the previous literature

[5]The accuracy of the classic Amihud measure has been documented for stocks (Hasbrouck, 2009) and currencies (Ranaldo and Santucci de Magistris, 2022). Fong et al. (2018) analyze global and U.S. stocks applying various liquidity proxies based on volatility over volume.

[6]Collin-Dufresne and Fos (2016) propose an elegant extension of Kyle's model, with which our model shares the stochastic nature of market liquidity.

on low- and high-frequency measurement of market liquidity, which has been predominantly based on the estimation of transaction costs rather than price impact.[7]

The manuscript is organized as follows. Section 2 outlines the theoretical setting. Section 3 reports the results of several Monte Carlo simulations. Section 4 introduces the notion of information jumps and of the jump-robust realized Amihud. Section 5 presents the empirical analysis, while Section 6 concludes the paper. Proof and additional empirical results are in the Appendix.

2 A Simple Theory of Illiquidity Measurement

Let us consider an asset traded on a market consisting of a finite number $J \geq 2$ of active participants. Within a given trading period of a certain unit length (e.g., an hour, a day, a week), the market passes through a sequence of $i = 1, \ldots, I$ equilibria. The evolution of the equilibrium price is motivated by the arrival of new information to the market that changes the reservation prices of the traders. At intra-period i, the exchanged quantity by the j-th trader is given by

$$q_{i,j} = \ell_i(\Delta p^*_{i,j} - \Delta p_i), \quad \ell_i > 0, \quad j = 1, \ldots, J, \tag{1}$$

where $\Delta p^*_{i,j}$ is the variation in the reservation log-price of the j-th trader occurring between period $i-1$ and period i. Similarly, Δp_i is the variation in the market log-price occurring in the same interval. The term ℓ_i is a positive coefficient capturing the market depth at time i: The larger the ℓ_i, the larger quantities of the asset can be exchanged for a given difference $\Delta p^*_{i,j} - \Delta p_i$. The equilibrium function in (1) is analogous to the one outlined in Tauchen and Pitts (1983), which provides a stylized representation of the supply-demand mechanism on the market.[8] The reservation price of each trader might reflect some of the following aspects: individual preferences, liquidity issues, asymmetries in information sets, and different expectations about the fundamental values of the asset. In general, the reservation price can deviate from the market price because of idiosyncratic reasons, inducing the j-th trader to trade. The quantity exchanged for a unit change of $\Delta p^*_{i,j} - \Delta p_i$ is given by the slope ℓ_i. In other words, ℓ_i measures the capacity of the market to allow large quantities to be exchanged at the intersection between demand and supply, thus recalling the concept of market depth and resilience that reduces the price impact of trading. The baseline assumptions of the model (linearity of the trading function and constant number of active traders) are inevitably stylized. As for the form of the equilibrium function in (1), note that the trades take place on short intra-period intervals of length $\delta = 1/I$ and are generally associated with small price variations. Therefore, it is not restrictive to assume the equilibrium function is linear on small price changes and for a fixed number of traders during such a short period.

By market clearing, that is $\sum_j q_{i,j} = 0$, we have that the average of the variations in the reservation prices clears the market, that is, $\Delta p_i = \frac{1}{J}\sum_{j=1}^{J} \Delta p^*_{i,j}$. As new information arrives, traders adjust their reservation prices, $\Delta p^*_{i,j}$, resulting in a change in the market price (Δp_i), which is given by the average

[7] Starting from the seminal work of Roll (1984), several papers propose other measures that estimate the bid-ask spread, including Hasbrouck (2009), Corwin and Schultz (2012), and Abdi and Ranaldo (2017).

[8] See also Clark (1973), Epps and Epps (1976), the survey in Karpoff (1987) and the empirical analysis in Andersen (1996).

of the increments of the reservation prices.

The generated trading volume in each i-th sub-interval $v_i = \frac{1}{2}\sum_{j=1}^{J} |q_{i,j}|$ is as follows

$$v_i = \frac{\ell_i}{2} \sum_{j=1}^{J} |\Delta p^*_{i,j} - \Delta p_i|, \tag{2}$$

We assume that the reservation price of each trader evolves in continuous-time according to the following process

$$dp^*_j(t) = \mu_j(t)dt + \sigma_j(t)dW_j(t), \quad j = 1, \ldots, J, \quad t > 0, \tag{3}$$

where $\{W_j(t), j = 1, \ldots J\}$ is a collection of independent Wiener processes. The term $\mu_j(t)$ is a predictable process with finite variation that might represent the long-term expectation of the j-th trader about the asset and could be a function of fundamental quantities, such as interest rates and macroeconomic variables. The term $\sigma_j(t)$ is the stochastic (spot) volatility process of the j-th trader. By letting σ_j vary across traders, we introduce *heterogeneity* among them. This reconciles with many realistic features, including the evidence of long-memory in volatility, as obtained by the superposition of traders operating at different frequencies, which, for instance, can be seen with the heterogeneous autoregressive models of Müller et al. (1997) and Corsi (2009). On the i-th discrete sub-interval of length $\delta = \frac{1}{I}$, the reservation prices for the j-th trader is therefore

$$\Delta p^*_{i,j} = \int_{\delta(i-1)}^{\delta i} \mu_j(s)ds + \int_{\delta(i-1)}^{\delta i} \sigma_j(s)dW_j(s). \tag{4}$$

This setting is coherent with a representation of a frictionless market where each trader participates through its reservation price to the determination of a new equilibrium. In particular, we assume that $\sigma_j(t) > 0$ is càdlàg with (almost surely) square integrable sample paths $\forall j = 1, \ldots, J$. Analogously, $\ell(t)$ evolves in continuous-time according to a process fulfilling very mild regularity conditions, i.e. $\ell(t)$ is assumed to be a strictly positive càdlàg stochastic process. For instance, examples of stochastic differential equation (SDE) fulfilling these conditions are those common in the volatility literature, such as the CIR model of Cox et al. (2005) and Heston (1993) (see Section 3), the Ornstein–Uhlenbeck process of Vasicek (1977), or the long-memory process of Comte and Renault (1998).

We define the *realized Amihud* as follows

$$\mathcal{A} := \frac{RPV}{v}, \tag{5}$$

where the numerator is the *realized power variation* of order one (or realized absolute variation), $RPV = \sum_{i=1}^{I} |r_i|$, where $r_i = \Delta p_i$ is the log-return, see Barndorff-Nielsen and Shephard (2003). The daily version by Amihud (2002) corresponds to the specific case with $I = 1$, i.e. the numerator reduces to the daily absolute return. Then, it should be evident that the classic daily Amihud is a special case of a more general metrics based on a richer set of intra-period information. Specifically, the realized Amihud gauges the price impact of trading, that is, the amount of volatility on a unit interval (as measured by RPV) associated with the trading "dollar" volume $v = \sum_{i=1}^{I} v_i$ generated in the same period.

In other words, $\mathcal{A}$ measures the amount of volatility associated with a unit of trading volume.[9] The following proposition highlights the main determinants of realized Amihud as an illiquidity measure.

Proposition 1. *Consider the illiquidity measure defined in (5), the equilibrium relation in (1), and the diffusive process for reservation prices in (3). Assume that $\sigma_j(t)$ and $\ell(t)$ are strictly positive càdlàg processes with (almost surely) square integrable sample paths $\forall j = 1, \ldots, J$. Assume $J = 2$ active traders, as representative of the two aggregated sides of the market. As $I \longrightarrow \infty$ (i.e., $\delta \longrightarrow 0$)*

$$p \lim_{I \to \infty} \mathcal{A} = \frac{1}{\mathcal{L}}, \tag{6}$$

where $\mathcal{L} = \int_0^1 \ell(s)ds$ is the integrated liquidity. Furthermore, as $I \longrightarrow \infty$

$$\frac{\log(\mathcal{A}) - \log\left(\frac{1}{\mathcal{L}}\right)}{\sqrt{\frac{2\delta(\pi/2-1)RV}{(\pi\delta/2)RPV^2}}} \xrightarrow{d} N(0,1), \tag{7}$$

where $RV = \sum_{i=1}^{I} r_i^2$ is the realized variance.

Proof. Proof in Appendix A.1. □

Proposition 1 shows that the realized Amihud is a measure of the inverse of the integrated liquidity $\mathcal{L}$, namely the *integrated illiquidity*, which represents the price impact of trading volume cumulated over periods of unit length. The precision of the measurement increases with I and the asymptotic distribution in (7) can be used to construct a confidence interval for $\mathcal{L}$. In the model of Clark (1973), Epps and Epps (1976) and Tauchen and Pitts (1983), volatility and trading volume (often used as a proxy for liquidity) are equilibrium outcomes of information impact and jointly depend upon the unobservable information flow variable, which generates variations in the reservation prices. By taking the ratio between volatility and volume, we decouple the information about market illiquidity from that of the information flow. Hence, by computing $\mathcal{A}$ over disjoint periods of unit length (e.g. on daily horizons), one can obtain a time-series of measurements of $\frac{1}{\mathcal{L}}$, and use them to explore the evolution of illiquidity over time (see Section 5). In the next section, we run Monte Carlo simulations to assess the finite sample performance of the realized Amihud in measuring illiquidity.

3 Monte Carlo Simulations

By resorting to the continuous-time framework outlined in Barndorff-Nielsen and Shephard (2002a,b), we can precisely measure the variability of the asset price by computing *RPV* over intervals of any length (e.g., hours, days, weeks, and months). Furthermore, the equilibrium theory presented above allows us to relate this variability to the aggregate level of disagreement among investors, in turn leading to the observed trading volume. An assessment of the quality of the measurement of illiquidity based on the realized Amihud is carried out by Monte Carlo simulations, in which the daily

[9] By analogy with the realized Amihud, one could employ the *realized Amivest*, which is defined as the reciprocal of the realized Amihud (the ratio of volume over volatility) that gives the volume of trading associated with a one standard deviation change in the price of a security.

horizon is taken as the reference unit interval. The liquidity process, $\ell(t)$, is generated according to a CIR-type SDE

$$d\ell(t) = \kappa_\ell(\ell(t) - \ell_0)dt + \eta_\ell \ell(t)^{1/2} dW_\ell(t),$$

where $\ell_0 = 50, 200, 500$ represents the long-term mean in the low-, medium-, and high-liquidity scenarios, respectively. The parameters $\kappa_\ell = 0.5$ and $\eta_\ell = 0.1$ determine the speed of the mean-reversion and the volatility of liquidity, respectively. Similarly, also the reservation prices (and, hence, equilibrium prices) are generated according to the diffusive process in (3), where the variance, $\sigma_j^2(t)$ with $j = 1, 2$, evolves following the dynamics of the CIR process, that is, $d\sigma_j^2(t) = \kappa_\sigma(\sigma^2(t) - \sigma_0^2)dt + \eta_\sigma \sigma(t) dW_{\sigma,j}(t)$ with the parameters $\kappa_\sigma = 0.2$, $\sigma_0^2 = 2$, $\eta_\sigma = 0.1$.[10] In the simulation of price and volume trajectories, we consider $M = 1000$ Monte Carlo replications for $T = 1,000$ transaction days and $I^* = 5,760$ intra-daily intervals corresponding to a 15-second frequency over 24 hours. *RPV* is then computed aggregating at daily horizon the absolute returns sampled at different frequencies: 1 hour; 30, 15, 10, 5 minutes; and 30 and 15 seconds, that is $I = [24, 48, 96, 144, 288, 1440, 2880, 5760]$ equally-spaced sub-intervals, respectively. Trading volume is obtained aggregating at daily horizon the volume generated in each sub-period according to equation (2). Hence, for each Monte Carlo simulation and for each sampling frequency, we obtain a time-series of realized Amihud $\{\mathcal{A}_t\}_{t=1}^T$ that we compare with the simulated time-series of integrated illiquidity, $\{\frac{1}{\mathcal{L}_t^*}\}_{t=1}^T$, where $\mathcal{L}_t^* = \sum_{i=1}^{I^*} \ell_{i,t}$, $t = 1, \ldots, T$.

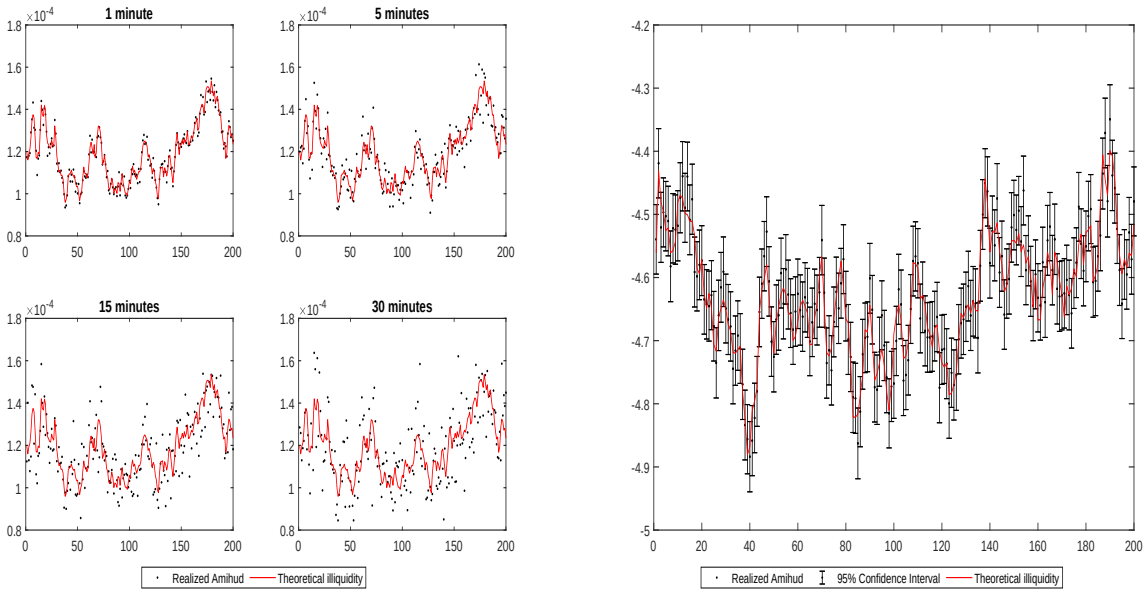

Figure 2: The realized Amihud at different frequencies and confidence intervals. The figure on the left reports the true illiquidity limit $\frac{1}{\mathcal{L}}$ (red solid line), and the realized Amihud (dots) obtained by sampling returns at different frequencies of 1 minute, 5, 15 and 30 minutes for a subset of 200 days. The figure on the right reports the true illiquidity signal ($\log \mathcal{L}$, red) and 95% confidence bands based on the realized Amihud computed with 1-minute returns.

[10] The configuration of these parameters generates a persistent volatility process with daily percentage returns typically ranging in the interval between -3% and +3%. In line with the empirical evidence displayed in Section 5, the simulated liquidity process $\ell(t)$ also displays a persistent behavior.

As a graphical illustration of the ability of the realized Amihud to precisely measure the latent illiquidity process, the left panel of Figure 2 reports the time-series of the daily true illiquidity signal (in red) together with its estimates (blue dots) that are the realized Amihud obtained by sampling at different frequencies (1 minute, 5, 15 and 30 minutes). As the sampling frequency increases, the variability around the true illiquidity signal decreases, and it becomes negligible at the 1-minute frequency. In other words, by taking the ratio between a increasingly refined (in I) measurement of daily volatility and daily trading volume, we obtain a very precise measurement of the day-by-day variations of the trade impact, which is a relevant dimension of illiquidity. The graph to the right of Figure 2 exploits the asymptotic distribution result in Proposition 1 and reports the 95% confidence bands around the true (log) illiquidity signal. The true illiquidity series lies within the confidence bands, thus confirming the goodness of the asymptotic approximation in (7). As a further illustration of asymptotic distribution of the realized Amihud, we construct quantile-quantile (QQ-) plots based on equation (22). Figure 3 reports the QQ-plots based on the simulation experiment described above, where $I = 24, 76, 288, 1440$. As I increases, the fit to the Gaussian distribution improves, being already remarkable at 5-minute frequencies.

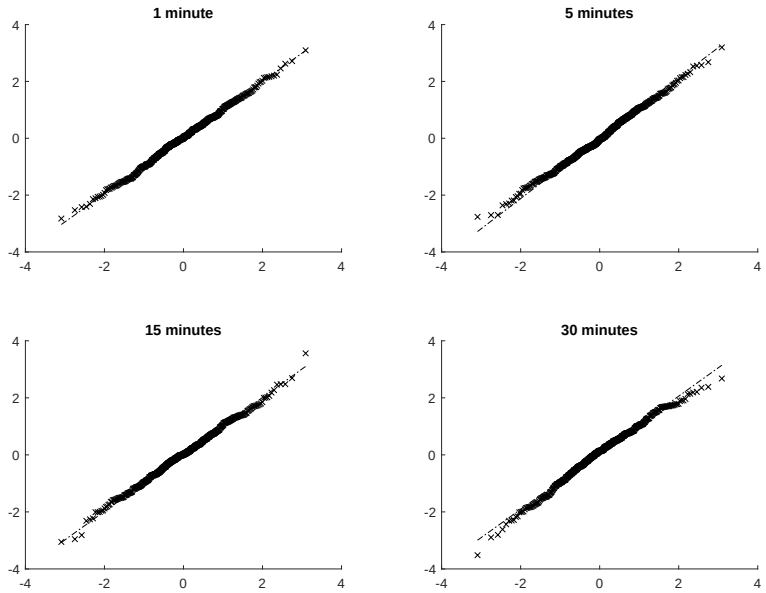

Figure 3: QQ-plot. Figure reports the QQ-plots and illustrates the approximation to a standard Gaussian random variable as in (7). We consider different sampling frequencies, namely 1 minute, 5 and 15 minutes, and 1 hour.

The summary of the results of the Monte Carlo simulations are presented in Table 1. The realized Amihud provides accurate measurements of the true integrated illiquidity process (i.e., $\frac{1}{\mathcal{L}}$) in all scenarios (low-, medium-, and high-illiquidity levels) with a bias (relative to the illiquidity signal) below 0.5% in absolute value and a small RMSE, even for relatively moderate sampling frequencies (e.g., 5-10 minutes). As expected from Theorem (1), the RMSE decreases as I increases (i.e., δ decreases). In general the RMSE of the realized Amihud is much smaller compared with the RMSE achieved by the daily Amihud. This result confirms that the classic daily Amihud represents the limiting case of

an illiquidity measurement obtained with only one observation per trading period, that is, $I = \delta = 1$. In this case, the illiquidity measure in (5) reduces to $\mathcal{A}^D = \frac{|r|}{v}$.

We consider an alternative low-frequency version of the daily Amihud, that is the *high-low Amihud*. We obtain it by exploiting the high-low price range as a proxy of volatility, see Parkinson (1980), among others. In particular, the high-low Amihud is defined as $\mathcal{A}^{HL} = \frac{range}{v}$, where $range = \sqrt{\frac{1}{4\log(2)}(p^H - p^L)^2}$ with p^H and p^L being the daily high and low log-prices on a given unit interval (a day in this case). The Monte Carlo simulations show that the high-low Amihud displays remarkable properties. It is characterized by a small negative bias (around 5%) and is approximately three times more efficient than the traditional daily Amihud. This suggests that the high-low Amihud constitutes a viable alternative to the daily Amihud when intra-day prices are not available.

Low Liquidity, $\ell_0 = 50$						
	Percentage Relative Bias			Relative RMSE		
Sampling frequency	Realized Amihud	High-Low Amihud	Daily Amihud	Realized Amihud	High-Low Amihud	Daily Amihud
1hour	1.6445	-5.5453	-2.5699	0.2330	0.2924	0.7450
30min	0.4541	-5.5453	-2.5699	0.1504	0.2924	0.7450
15min	0.5667	-5.5453	-2.5699	0.1097	0.2924	0.7450
10min	-0.0095	-5.5453	-2.5699	0.0901	0.2924	0.7450
5min	0.2309	-5.5453	-2.5699	0.0614	0.2924	0.7450
1min	0.0923	-5.5453	-2.5699	0.0291	0.2924	0.7450
30sec	0.1065	-5.5453	-2.5699	0.0201	0.2924	0.7450
15sec	0.0630	-5.5453	-2.5699	**0.0142**	0.2924	0.7450
Medium Liquidity, $\ell_0 = 200$						
	Percentage Relative Bias			Relative RMSE		
Sampling frequency	Realized Amihud	High-Low Amihud	Daily Amihud	Realized Amihud	High-Low Amihud	Daily Amihud
1hour	3.6035	-3.9223	-2.4906	0.2326	0.2934	0.7547
30min	2.2201	-3.9223	-2.4906	0.1581	0.2934	0.7547
15min	0.5300	-3.9223	-2.4906	0.1084	0.2934	0.7547
10min	0.6963	-3.9223	-2.4906	0.0874	0.2934	0.7547
5min	0.2997	-3.9223	-2.4906	0.0615	0.2934	0.7547
1min	0.0216	-3.9223	-2.4906	0.0277	0.2934	0.7547
30sec	-0.0456	-3.9223	-2.4906	0.0194	0.2934	0.7547
15sec	0.0045	-3.9223	-2.4906	**0.0139**	0.2934	0.7547
High Liquidity, $\ell_0 = 500$						
	Percentage Relative Bias			Relative RMSE		
Sampling frequency	Realized Amihud	High-Low Amihud	Daily Amihud	Realized Amihud	High-Low Amihud	Daily Amihud
1hour	3.1471	-6.4177	-4.7968	0.2330	0.2918	0.7575
30min	1.6101	-6.4177	-4.7968	0.1616	0.2918	0.7575
15min	0.8523	-6.4177	-4.7968	0.1096	0.2918	0.7575
10min	0.6709	-6.4177	-4.7968	0.0898	0.2918	0.7575
5min	0.2646	-6.4177	-4.7968	0.0634	0.2918	0.7575
1min	0.0035	-6.4177	-4.7968	0.0279	0.2918	0.7575
30sec	0.0655	-6.4177	-4.7968	0.0200	0.2918	0.7575
15sec	0.0598	-6.4177	-4.7968	**0.0146**	0.2918	0.7575

Table 1: Illiquidity measurement. The table reports Monte Carlo simulations for the assessment of the quality of illiquidity through the realized Amihud. It also reports the Monte Carlo relative percentage bias and RMSE (both relative to $\frac{1}{\mathcal{L}}$) for the realized Amihud reported in (5). The smallest RMSE is in bold. As a reference, we also consider the daily Amihud measure, that is, $\mathcal{A}^D = \frac{|r|}{v}$, and the high-low Amihud, $\mathcal{A}^{HL} = \frac{range}{v}$, where *range* is scaled by $\sqrt{\pi/2}$ to be comparable with the *RPV*.

3.1 Microstructure Frictions

It should be stressed that the asymptotic results (in the limit for $I \to \infty$) behind Proposition 1 are derived by abstracting from microstructure frictions (namely *microstructure noise*), like transaction costs in the form of bid-ask spread, clearing fees, or price discreteness, which are intimately related

and endogenous to the trading process. Although in the simplified context provided by the model these microstructure features are not explicitly included, they pose a relevant issue to be addressed in the empirical analysis. From a statistical point of view, the microstructure noise dominates the volatility signal as $I \to \infty$, thus leading to distorted measurements of the variance. In the literature on realized variance it is common practice to resort to moderate sampling frequencies, for example, 5-minute intervals, to reduce the impact of the microstructure noise contamination on the volatility measurement, see Aït-Sahalia and Jacod (2014) and Liu et al. (2015) for a discussion.[11] This approach can be carried over to the illiquidity measurement, and its effectiveness in reducing the impact of microstructure noise contamination is confirmed by the evidence reported in Table 2. In particular, we repeat the analysis of Table 1, but this time, we add the bid-ask spread to the equilibrium prices and consider a rounding mechanism that generates price discreetness (rounding to cents or decimalization effect) and zero returns; for more, see Bandi et al. (2020), among others.[12]

The results in Table 2 deliver two main messages. First, it suggests that, in this setting, we should avoid computing the realized Amihud by sampling at the highest possible frequencies (e.g., from 15 to 30 seconds) because this leads to large estimation biases. Instead, sampling at moderate frequencies (e.g., from 5 to 10 minutes) drastically reduces the bias while also leading to a low RMSE, especially if compared with the daily Amihud, which is about 10 times larger (0.069 compared with 0.733 for the medium liquidity scenario). Second, the realized Amihud measure also performs well in a low liquidity setting suggesting that its accuracy remains high for less frequently traded financial securities.

In summary, the realized Amihud based on 5-minute returns provides accurate measurements of the illiquidity associated with the price impact even in settings characterized by other dimensions of illiquidity: the transaction costs such as the bid-ask spread, and additional frictions such as staleness due to inherent price discreetness and absence of new information. In the empirical analysis below, we work assuming that sampling asset returns at 5-minute intervals is sufficient to achieve a precise measurement of the asset illiquidity.

4 Information Jumps

Now, we further explore the relationship between liquidity and volatility, focusing on the arrival of large news common to all traders. Note that the increments of the reservation log-prices can be disentangled as follows

$$\Delta p^*_{i,j} = \phi_i + \psi_{i,j}, \quad \text{with} \quad j = 1, \dots, J,$$

[11] Alternative techniques designed to directly tackle the microstructural features in the measurement of volatility based on intra-daily returns are: the two-scales estimator of Zhang et al. (2005) based on the idea of subsampling, the optimal sampling frequency method of Bandi and Russell (2008), the realized kernel by Barndorff-Nielsen et al. (2008), the pre-averaging estimator of Podolskij and Vetter (2009). In a large scale empirical analysis, Liu et al. (2015) find little evidence that the realized variance estimator based on returns sampled at 5-minutes frequencies is outperformed by the other measures.

[12] The bid-ask mechanism on the observed log-price is generated as $\tilde{p}_i = p_i + \zeta_i \cdot BAS/2$, where BAS is the bid-ask spread and ζ_i is an i.i.d. random variable (independent of p_i) taking value 1 or -1 with equal probability. The decimalization mechanism is then imposed on $\tilde{p}_i$ by rounding $\tilde{P}_i = \exp(\tilde{p}_i)$ to the closest cent.

Low Liquidity, $\ell_0 = 50$						
	Percentage Relative Bias			Relative RMSE		
Sampling frequency	Realized Amihud	High-Low Amihud	Daily Amihud	Realized Amihud	High-Low Amihud	Daily Amihud
1hour	1.8020	-4.8748	-0.7818	0.2176	0.3054	0.7711
30min	1.8298	-4.8748	-0.7818	0.1569	0.3054	0.7711
15min	1.6781	-4.8748	-0.7818	0.1151	0.3054	0.7711
10min	1.7789	-4.8748	-0.7818	0.0921	0.3054	0.7711
5min	2.9765	-4.8748	-0.7818	**0.0725**	0.3054	0.7711
1min	13.3029	-4.8748	-0.7818	0.1476	0.3054	0.7711
30sec	25.1862	-4.8748	-0.7818	0.2720	0.3054	0.7711
15sec	28.4629	-4.8748	-0.7818	0.3149	0.3054	0.7711
Medium Liquidity, $\ell_0 = 200$						
	Percentage Relative Bias			Relative RMSE		
Sampling frequency	Realized Amihud	High-Low Amihud	Daily Amihud	Realized Amihud	High-Low Amihud	Daily Amihud
1hour	2.9646	-4.8349	-1.9522	0.2258	0.2812	0.7334
30min	1.5911	-4.8349	-1.9522	0.1587	0.2812	0.7334
15min	1.5683	-4.8349	-1.9522	0.1110	0.2812	0.7334
10min	1.8408	-4.8349	-1.9522	0.0930	0.2812	0.7334
5min	2.6054	-4.8349	-1.9522	**0.0690**	0.2812	0.7334
1min	12.0901	-4.8349	-1.9522	0.1276	0.2812	0.7334
30sec	22.9034	-4.8349	-1.9522	0.2355	0.2812	0.7334
15sec	25.5046	-4.8349	-1.9522	0.2640	0.2812	0.7334
High Liquidity, $\ell_0 = 500$						
	Percentage Relative Bias			Relative RMSE		
Sampling frequency	Realized Amihud	High-Low Amihud	Daily Amihud	Realized Amihud	High-Low Amihud	Daily Amihud
1hour	1.8504	-5.9370	-1.3766	0.2463	0.2818	0.7248
30min	0.9157	-5.9370	-1.3766	0.1640	0.2818	0.7248
15min	0.9431	-5.9370	-1.3766	0.1097	0.2818	0.7248
10min	1.1633	-5.9370	-1.3766	0.0892	0.2818	0.7248
5min	2.2907	-5.9370	-1.3766	**0.0676**	0.2818	0.7248
1min	8.9761	-5.9370	-1.3766	0.0964	0.2818	0.7248
30sec	16.9324	-5.9370	-1.3766	0.1736	0.2818	0.7248
15sec	17.0739	-5.9370	-1.3766	0.1764	0.2818	0.7248

Table 2: Illiquidity measurement with microstructure noise. The table reports Monte Carlo simulations for assessing the quality of illiquidity through the realized Amihud. The bid-ask spread is set at 0.15% relative to the price level, which in line with the observed relative bis-ask spread of SPY (see Section 5). Table reports the Monte Carlo relative percentage bias and RMSE (both relative to $\frac{1}{\mathcal{L}}$) for the realized Amihud reported in (5). The smallest RMSE is in bold. As a reference, we also consider the daily Amihud measure, that is, $\mathcal{A}^D = \frac{|r|}{v}$, and the high-low Amihud, $\mathcal{A}^{HL} = \frac{range}{v}$, where $range$ is scaled by $\sqrt{\pi/2}$ to be comparable with the RPV.

where ϕ_i represents a fundamental information component common to all traders, stemming from public information events, such as those associated with earnings press releases or central banks' announcements. This could be related to events that trigger common directional beliefs among practitioners. The term $\psi_{i,j}$ is the change in the discretized diffusive process outlined in (2), which represents the investor's specific component of the reservation price variation. Furthermore, the assumption of independence between ϕ_i and $\psi_{i,j}$ across time and traders does not allow for reversal or spillover effects, such as those studied in Grossman and Miller (1988) to investigate the mechanics of liquidity provision. The same type of sequential trading behavior has been recently proven to be responsible for crash episodes, as shown in Christensen et al. (2022), and associated with changes in the level of investors' disagreement around important news announcements, see, e.g., Bollerslev et al., 2018.[13] The detection of such informational events needs an accurate identification econometric technique and granular (intra-daily) data.

The recent advances in the literature on *jump* processes help in this analysis. Similarly to Bollerslev et al. (2018), we rely on a simple setup for the common news component, to separately identify it

[13] Perraudin and Vitale (1996) also consider jump times as moments at which significant information becomes public knowledge.

from the component of price variation due to the disagreement among traders, which is responsible for generating the trading volume.[14] For this reason, we refer to the term ϕ_i as *information jumps*. In other words, when a common large news hits the market, the reservation prices all change in the same direction, thus leading to a new equilibrium price. This generates price volatility with little or no associated trading volume, so the realized Amihud is expected to be subject to a large positive shock. Ideally, we would like to disentangle this spike from the measurement of illiquidity related with the disagreement among traders.

We rely upon the theory of multipower variation developed in Barndorff-Nielsen and Shephard (2003, 2004, 2006) to carry out inference on information jumps in illiquidity. Following Barndorff-Nielsen and Shephard (2006), we assume that ϕ_i is a compound Poisson process, namely $\phi_i = \sum_{j=1}^{\mathcal{N}_i} c_j$, where $\mathcal{N}_i$ is a simple process (e.g., a Poisson) that counts the number of jump arrivals in the interval $[i-1, i]$, and it is finite for all intervals i. The terms c_j are nonzero random variables that determine the size of the jumps. When $\mathcal{N}_i = 0$, then $\Delta p^*_{i,j}$ reduces to the stochastic volatility plus drift model, whose dynamics are described in (3). To carry out inference on jumps, we consider the multipower variation of order $1/2$, namely

$$MPV = \frac{I}{I-1} \sum_{i=2}^{I} |r_i|^{1/2} |r_{i-1}|^{1/2}. \tag{8}$$

Following Barndorff-Nielsen and Shephard (2004, 2006), MPV converges to $\mathcal{S}$, even when $\phi_i \neq 0$, that is

$$p \lim_{I \to \infty} \delta^{1/2} \mu_{1/2}^{-2} MPV = \mathcal{S}, \tag{9}$$

where $\mu_{1/2} = E[|X|]^{1/2}$ is a normalizing constant. Therefore, we can devise the jump test statistic, $\mathcal{J}$, which is given by

$$\mathcal{J} = \frac{\sqrt{\pi/2}\mu_{1/2}^2 RPV - MPV}{\widetilde{BPV}}, \tag{10}$$

where $\widetilde{BPV} = \sqrt{\xi \sum_{i=2}^{I} |r_i||r_{i-1}|}$ and $\xi = \theta(\mu_1^2 + 2\mu_{1/2}^2\mu_1 - 3\mu_{1/2}^4)/\mu_1^2)$ is a scaling constant with $\theta = 0.1032$. Under the null hypothesis that $\phi_i = 0$, $\mathcal{J} \xrightarrow{d} N(0,1)$, we can use this result for testing the presence of a significant information jump in a given day. With the goal of wiping out the impact of information jumps on $\mathcal{A}$, we can construct the *jump-robust* realized Amihud as

$$\mathcal{A}^C = \frac{RPV_C}{\nu}, \tag{11}$$

where RPV_C is the jump-robust realized power variation, given by

$$RPV_C = \mathbb{I}(\mathcal{J} \leq q_{1-\alpha}) RPV + \mathbb{I}(\mathcal{J} > q_{1-\alpha}) \widetilde{MPV}, \tag{12}$$

where $\mathbb{I}(\cdot)$ is the indicator function, $q_{1-\alpha}$ denotes the $(1-\alpha)$-th quantile of a standard Gaussian distribution, α is the significance level of the jump test, and $\widetilde{MPV} = \sqrt{2/\pi}\mu_{1/2}^{-2} MPV$.

[14] Other studies associating large price jumps with news announcements can be found in Andersen et al. (2007),

Low Liquidity	Power			Size		
	5%	1%	0.5%	5%	1%	0.5%
1h	79.83%	75.35%	73.80%	10.31%	4.69%	3.52%
30min	84.71%	80.85%	79.55%	8.48%	3.16%	2.18%
15min	86.97%	83.54%	82.56%	7.68%	2.51%	1.56%
10min	88.83%	85.83%	84.40%	6.65%	2.02%	1.29%
5min	90.55%	87.55%	86.48%	6.25%	1.77%	1.10%
1min	92.67%	90.19%	89.16%	5.63%	1.35%	0.77%
30sec	93.35%	90.71%	89.77%	5.72%	1.33%	0.69%
15sec	93.52%	91.45%	90.67%	5.44%	1.18%	0.63%
Medium Liquidity	Power			Size		
	5%	1%	0.5%	5%	1%	0.5%
1h	79.87%	75.46%	73.96%	10.70%	4.89%	3.69%
30min	85.06%	81.18%	79.60%	8.72%	3.42%	2.31%
15min	87.82%	84.48%	83.05%	7.07%	2.42%	1.54%
10min	89.16%	86.04%	84.94%	6.98%	2.29%	1.30%
5min	90.47%	87.56%	86.65%	6.53%	1.92%	1.05%
1min	92.86%	90.29%	89.55%	5.66%	1.24%	0.68%
30sec	93.13%	90.97%	90.05%	5.47%	1.38%	0.81%
15sec	93.59%	91.15%	90.48%	5.77%	1.35%	0.73%
High Liquidity	Power			Size		
	5%	1%	0.5%	5%	1%	0.5%
1h	80.24%	76.05%	74.22%	10.48%	5.10%	4.10%
30min	84.04%	80.22%	78.79%	8.53%	3.32%	2.31%
15min	87.96%	84.13%	82.89%	7.51%	2.54%	1.64%
10min	89.04%	85.32%	84.49%	6.86%	2.23%	1.43%
5min	90.59%	88.03%	86.67%	6.46%	1.87%	1.12%
1min	92.40%	90.14%	89.25%	5.67%	1.29%	0.67%
30sec	93.22%	91.00%	90.02%	5.45%	1.35%	0.71%
15sec	93.69%	91.52%	90.64%	5.35%	1.21%	0.69%

Table 3: Jump test: power and size. The table reports Monte Carlo simulations for the assessment of the power and size of the jump test. The empirical size and power of the jump test are computed at the 5%, 1%, and 0.5% theoretical size levels, respectively.

In the following, we study by Monte Carlo simulations the finite-sample size and power properties of the $\mathcal{J}$-test. In Table 3 we consider a frictionless setting and three levels of nominal size, namely $\alpha = 5\%, 1\%, 0.5\%$. The best performance in terms of empirical size and power is achieved sampling at the highest possible frequency of 15-seconds. Furthermore, considering a setting where $\phi_i \neq 0$ allows us to study the power of the test, that is, the ability to identify a jump if it occurs. In particular, we assume that ϕ_i follows a compound Poisson process with an intensity equal to 5% (one jump every twenty days on average). Notably, the test correctly identifies jumps, that is, rejects the null hypothesis of no jumps, in more than 90% of the cases when sampling at the highest frequencies.

The results are quite different when considering microstructure noise, in the form of bid-ask

Chaboud et al. (2008), Lee (2011), Jiang et al. (2011).

spread and rounding effects (Table 4). In particular, rounding to the closest cent of the dollar generates a large number of zeros in the returns sampled at the highest frequencies, as shown by Bandi et al. (2020). Kolokolov and Renò (2021) illustrate the detrimental effect of zeros on the quality of the jump-robust volatility estimates, especially when power variation measures are adopted. In circumstances where zeros are the dominant feature of the high-frequency returns (like for very illiquid stocks), the effect of the rounding on *MPV* is detrimental. In this case, *MPV* is associated with a large negative bias, and the jump test rejects the null hypothesis very frequently. In this case, sampling at 10 to 15 minutes frequencies drastically reduces the bias in *MPV*, thus leading to empirical sizes of the jump test closer to the theoretical ones. At these frequencies, the power remains high and above 85% in all cases.

Low Liquidity	Power			Size		
	5%	1%	0.5%	5%	1%	0.5%
1h	80.99%	76.34%	74.43%	10.98%	5.08%	3.98%
30min	84.94%	81.39%	79.92%	10.78%	4.70%	3.32%
15min	88.59%	85.77%	84.44%	11.04%	4.64%	3.28%
10min	90.49%	87.41%	86.32%	12.26%	4.74%	3.16%
5min	93.07%	90.78%	89.83%	20.64%	8.82%	6.44%
1min	98.96%	98.22%	97.87%	97.62%	93.02%	90.92%
30sec	99.70%	99.45%	99.32%	100.00%	100.00%	100.00%
15sec	99.96%	99.96%	99.94%	100.00%	100.00%	100.00%
Medium Liquidity	Power			Size		
	5%	1%	0.5%	5%	1%	0.5%
1h	81.21%	76.91%	75.55%	10.72%	5.16%	3.90%
30min	86.53%	82.76%	81.48%	10.12%	4.48%	3.22%
15min	89.81%	86.61%	85.37%	12.22%	4.96%	3.48%
10min	90.74%	87.90%	86.92%	13.52%	5.52%	3.76%
5min	94.07%	91.53%	90.66%	24.08%	11.30%	8.14%
1min	99.74%	99.27%	99.13%	97.84%	94.36%	92.30%
30sec	100.00%	99.94%	99.92%	100.00%	100.00%	99.98%
15sec	99.98%	99.98%	99.98%	100.00%	100.00%	100.00%
High Liquidity	Power			Size		
	5%	1%	0.5%	5%	1%	0.5%
1h	80.04%	75.75%	73.89%	10.96%	5.00%	3.88%
30min	84.32%	80.17%	78.93%	8.94%	3.50%	2.44%
15min	88.67%	85.07%	83.44%	8.84%	3.06%	1.90%
10min	89.99%	86.88%	85.93%	8.54%	2.72%	1.64%
5min	93.05%	90.22%	89.17%	10.76%	4.00%	2.56%
1min	99.27%	98.59%	98.34%	56.15%	36.61%	30.07%
30sec	99.70%	99.62%	99.54%	97.88%	92.80%	89.72%
15sec	100.00%	99.92%	99.92%	100.00%	100.00%	100.00%

Table 4: Jump test: power and size with microstructure noise. The table reports Monte Carlo simulations for the assessment of the power and size of the jump test. The bid-ask spread is set at 0.15% relative to the price level. The empirical size and power of the jump test are computed at the 5%, 1%, and 0.5% theoretical size levels, respectively.

5 Empirical Analysis

We now illustrate how changes in the liquidity conditions of financial markets can be studied by looking at the temporal evolution of the realized illiquidity measures.[15] In particular, we consider the time series of the realized Amihud of SPDR S&P 500 ETF (ticker SPY), which is the ETF tracking the S&P 500 index, and of the EUR/CHF and USD/CHF foreign exchange (FX) rates. With a daily volume of 82.45 million shares in the period 2016–2021, SPY is the ETF with the largest trading volume in the world. For this reason, the realized Amihud of SPY can be considered a good proxy for the overall liquidity condition on the equity market. As for the EUR/CHF and USD/CHF rates, our intent is to consider another financial security with different characteristics, for example, the OTC and dealership structure as well as a price setting for which it is not obvious to expect the (illiquidity) leverage effect. The Swiss franc also provides us with an interesting laboratory, given the peculiar behavior of both volume and volatility after the cap removal by the Swiss national bank in January 2015. This circumstance makes it an interesting case study for assessing the evolution of price impact measures around policy events that change the currency policy and trading environment. The analysis of the stock market illiquidity is presented in Section 5.1, while Section 5.2 presents the results of the analysis conducted on the currency market.

5.1 Stock Market Illiquidity

We consider the daily time series of the realized Amihud of SPY, which is computed as the ratio between the daily *RPV* obtained from intra-daily returns sampled at different frequencies (source TAQ database) and the daily volume (expressed in dollars, source Bloomberg) on SPY for the period January 3, 2006, to June 29, 2018.

5.1.1 Sample Statistics

Table 5 reports the sample statistics of RPV, volume, $\mathcal{A}$ (realized Amihud), $\mathcal{A}^C$ (the jump-robust version), and the jump-component of the realized Amihud, computed as $\mathcal{A}_t^{\mathcal{J}} = \frac{\mathbb{I}(\mathcal{J}>q_{1-\alpha})(RPV-\widehat{MPV})}{v}$. The table also contains the sample statistics for the classic daily Amihud ($\mathcal{A}^D$) and of the high–low Amihud ($\mathcal{A}^{HL}$).[16] The series are computed using returns sampled at several frequencies (1, 5, 10, 15, and 30 minutes). In the last row, the table reports the number of significant jumps identified with the test in (10). As expected, the variability of the realized Amihud is much smaller than that of the daily Amihud (by about 9 or 10 times), and this holds irrespective of the sampling frequency used to compute the estimator. In turn, the variability of the $\mathcal{A}^{HL}$ is approximately three or four times lower than that of $\mathcal{A}^D$, reiterating that the range-based illiquidity measure is more desirable than daily Amihud when low-frequency illiquidity proxies are to be used. All series display positive skewness

[15] Another way to assess the accuracy of realized Amihud is to compare it with liquidity measures of price impact originating from order flow as done in Ranaldo and Santucci de Magistris (2022) showing that the realized Amihud is an accurate measure of FX volume price impact.

[16] To interpret these measures as the amount of daily price volatility associated with one dollar of trading volume, in the empirical application, we multiply $\mathcal{A}^D$ by the constant $\sqrt{\pi/2}$ and $\mathcal{A}$ by the constant $\delta^{1/2}\sqrt{\pi/2}$. This guarantees that $\mathcal{A}$, $\mathcal{A}^D$, and $\mathcal{A}^{HL}$ are on the same scale.

	Variance					
	1min	5min	10min	15min	30min	Daily
RPV	0.311	0.312	0.314	0.317	0.335	0.547
Volume	–	–	–	–	–	1.029
$\mathcal{A}$	2.433	2.420	2.427	2.491	2.722	–
$\mathcal{A}^{C}$	2.262	2.419	2.456	2.553	2.804	–
$\mathcal{A}^{\mathcal{J}}$	0.053	0.030	0.042	0.063	0.149	–
$\mathcal{A}^{D}$	–	–	–	–	–	9.541
$\mathcal{A}^{HL}$	–	–	–	–	–	3.755
	Skewness					
RPV	3.871	3.650	3.700	3.820	3.824	3.476
Volume	–	–	–	–	–	1.984
$\mathcal{A}$	1.306	1.294	1.200	1.152	1.038	1.245
$\mathcal{A}^{C}$	1.203	1.277	1.184	1.139	0.963	–
$\mathcal{A}^{\mathcal{J}}$	1.765	3.160	3.720	3.569	3.342	–
$\mathcal{A}^{HL}$	–	–	–	–	–	1.453
	Kurtosis					
RPV	28.728	24.426	25.352	26.867	26.072	22.381
Volume	–	–	–	–	–	8.839
$\mathcal{A}$	5.322	5.210	4.855	4.669	4.419	5.015
$\mathcal{A}^{C}$	4.942	5.210	4.889	4.696	4.115	–
$\mathcal{A}^{\mathcal{J}}$	7.741	13.490	18.639	18.161	16.162	–
$\mathcal{A}^{HL}$	–	–	–	–	–	6.497
# of significant jumps	1896	386	314	343	413	–

	Correlation Matrix						
	RPV	Volume	$\mathcal{A}$	$\mathcal{A}_t^{C}$	$\mathcal{A}^{\mathcal{J}}$	$\mathcal{A}^{D}$	$\mathcal{A}^{HL}$
RPV	–	0.8860	0.2264	0.2377	-0.1005	0.1171	0.1991
Volume	0.8470	–	-0.1498	-0.1356	-0.1272	0.0374	-0.0316
$\mathcal{A}$	0.2200	-0.2788	–	0.9937	0.0575	0.2250	0.6328
$\mathcal{A}^{C}$	0.2375	-0.2582	0.9906	–	-0.0544	0.2198	0.6215
$\mathcal{A}^{\mathcal{J}}$	-0.1568	-0.1267	-0.0470	-0.1680	–	0.0472	0.1015
$\mathcal{A}^{D}$	0.1109	0.0239	0.1510	0.1443	0.0328	–	0.6662
$\mathcal{A}^{HL}$	0.1830	-0.1340	0.5997	0.5892	0.0171	0.5917	–

Table 5: Descriptive statistics. The table reports the sample statistics for the *RPV*, daily volume, the realized Amihud ($\mathcal{A}$), the Amihud's jump-robust version ($\mathcal{A}^{C}$), the jump component ($\mathcal{A}^{\mathcal{J}}$), the classic daily Amihud ($\mathcal{A}^{\mathcal{D}}$), the high–low Amihud ($\mathcal{A}^{HL}$), as well as the number of significant jumps detected by the $\mathcal{J}$ test at the 1% significance level. The variance is scaled by a factor of E+04, while for the volume is scaled by a factor of E-16. In the bottom panel, the table reports the Pearson–Spearman (upper/lower triangular matrix) correlations.

and excess kurtosis compared with the reference value of the Gaussian distribution. Interestingly, the kurtosis of *RPV* is much larger than that of the realized Amihud. This suggests that *RPV* and trading volume tend to spike on the same days, so that dividing *RPV* by trading volume drastically reduces the

observed kurtosis. Finally, volatility and volume are strongly correlated (around 85%); a somewhat expected result. However, the correlations of $\mathcal{A}$ with *RPV* and trading volume are smaller, about 22% and -28% (Pearson), signaling that liquidity interrelates with volatility and trading volume, but still differs from them. The realized Amihud (computed with returns sampled at the 5-minute frequency) is positively correlated with both the daily and high–low Amihud. In particular, the correlation is much stronger with the latter, suggesting that $\mathcal{A}^{HL}$ is a more precise (or less noisy) measure of the illiquidity signal compared with $\mathcal{A}^{D}$.

Figure 4 displays the time series of the realized Amihud computed by employing returns sampled at the 5-minute frequency (black solid line), the daily Amihud (blue dotted line), and the high–low Amihud (yellow dashed line). Notably, the three series share very similar dynamic patterns, signaling that they are all nonparametric measurements of the same underlying stochastic quantity, that is the integrated illiquidity. However, the daily Amihud displays much more variability than the realized Amihud. Interestingly, the high–low Amihud, although being based on low-frequency data available at the daily horizon, displays a range of variability of an order close to that of the realized Amihud.

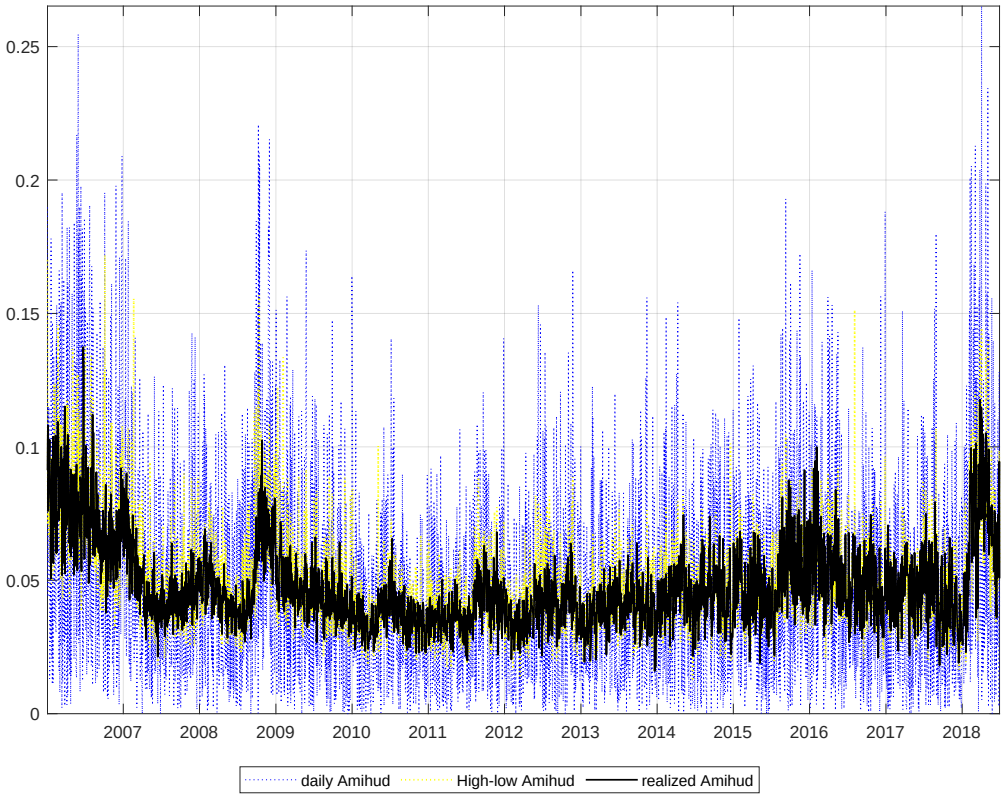

Figure 4: Illiquidity measurements. Realized Amihud (black solid line), daily Amihud (blue dotted line), and high–low Amihud (yellow dashed line) of SPY. Sample period: January 3, 2006 – June 29, 2018. Both series are scaled by a factor of E+09.

From a visual inspection of Figure 4 it also emerges that long periods with low illiquidity are followed by protracted periods of high illiquidity. Within the volatility literature, this is a well-established phenomenon known as *volatility clustering*. Because a similar pattern applies to the realized Amihud, we refer to it as *illiquidity clustering*. Figure 5 reports the empirical autocorrelation

function (ACF) of the daily and realized Amihud. The realized Amihud displays strong persistence, as measured by the slow decay rate of the ACFs that remain very high even after 50 lags, whereas the autocorrelation of the daily Amihud is much less persistent. Concerning the daily Amihud, this is the typical behavior of persistent time series contaminated by additive noise, as indicated, for instance, by Hurvich and Ray (2003) and Hurvich et al. (2005) in the context of stochastic volatility estimation. Altogether, the evidence outlined in Figures 4 and 5 suggest two points: First, it justifies the use of well-established volatility models for predicting illiquidity. Second, the strong persistence of an illiquidity shock has important implications in asset pricing.

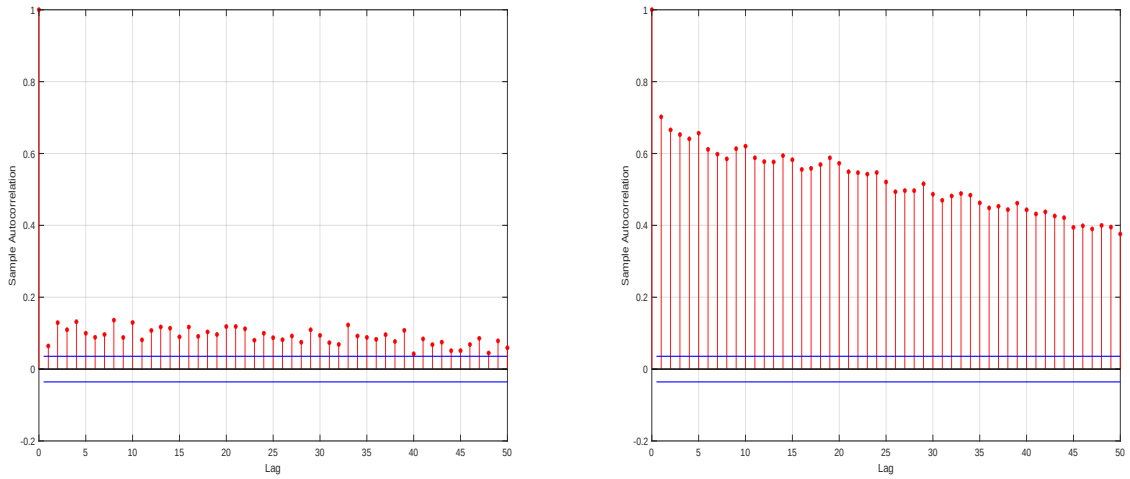

(a) Daily Amihud

(b) Realized Amihud

Figure 5: Autocorrelation. Empirical autocorrelation function of the daily Amihud (left panel) and of the realized Amihud (right panel).

Finally, Figure 6 reports prima-facie evidence on the relationship between negative returns and illiquidity. In particular, Figure 6 displays the increase (in relative terms) in the realized Amihud following a negative shock to returns for different time horizons, $s = 1, \ldots, 20$. Analogously, a positive shock to returns improves liquidity (or reduces illiquidity) for many periods. The main stylized fact emerging from Figure 6 is that past negative returns are associated with an increase in illiquidity in the subsequent periods. Furthermore, this effect is rather persistent, remaining significant after 15 periods. In particular, a negative return generates on average an increase in the realized Amihud of about 6% in the next day and a persistent increase of about 2% after two weeks.

5.1.2 Modeling Realized lliquidity

We consider both linear and nonlinear dynamic specifications for the realized Amihud to uncover the distributional characteristics of illiquidity and ascertain its superiority compared to traditional Amihud measure in capturing them. In particular, we consider a parametric model pertaining to the class of multiplicative error models (MEM) – as introduced by Engle (2002) and Engle and Gallo (2006). Inspired by the heterogenous autoregressive (HAR) model of Corsi (2009), we consider the

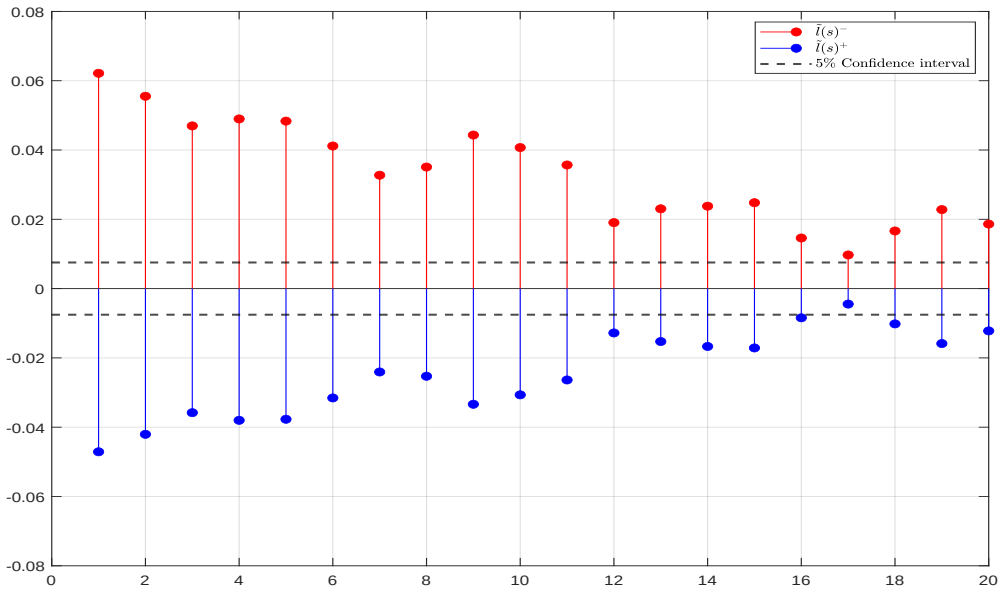

Figure 6: Illiquidity and negative/positive return shock propagation. Figure reports the estimated propagation of the effect of a negative (red bars) and positive (blue bars) shock on returns on the realized Amihud. Following Catania (2020), these quantities are computed as the empirical counterpart of $l^+(s) = E[\mathcal{A}_{t+s}|r_t > 0] - E[\mathcal{A}_{t+s}]$, $l^-(s) = E[\mathcal{A}_{t+s}|r_t < 0] - E[\mathcal{A}_{t+s}]$ for $s = 1, \ldots, 20$. The estimators $\hat{l}^+(s)$ and $\hat{l}^-(s)$ are reported relative to the average illiquidity, i.e. $\tilde{l}^+(s) = l^+(s)/E[\mathcal{A}_{t+s}]$ and $\tilde{l}^-(s) = l^-(s)/E[\mathcal{A}_{t+s}]$. The black-dashed horizontal lines denote the 95% interval around 0.

MEM-AHAR model,[17] as follows

$$\mathcal{A}_t = \mu_t \epsilon_t, \tag{13}$$

where μ_t is the conditional mean of the process, and it follows asymmetric HAR dynamics as

$$\mu_t = \omega + \alpha_d \mathcal{A}_{t-1} + \alpha_w \bar{\mathcal{A}}_{w,t-1} + \alpha_m \bar{\mathcal{A}}_{m,t-1} + \gamma D_{t-1} \mathcal{A}_{t-1}, \tag{14}$$

where $\bar{\mathcal{A}}_{w,t-1} = \frac{1}{5}\sum_{i=1}^{5} \mathcal{A}_{t-i}$, $\bar{\mathcal{A}}_{m,t-1} = \frac{1}{22}\sum_{i=1}^{22} \mathcal{A}_{t-i}$, and D_{t-1} is a dummy variable taking value of 1 if the return is negative and 0 otherwise; this accounts for an asymmetric response of illiquidity to positive or negative returns. Although with a different interpretation, this setting is reminiscent of the GJR-GARCH(1,1) model by Glosten et al. (1993) and it is supposed to capture the illiquidity *leverage* effect. The asymmetric mechanism would be consistent with the stronger illiquidity persistence originated from negative returns (Figure 6), empirical evidence provided in Hameed et al. (2010), and theoretical models of binding capital constraints of financial intermediaries (e.g. Brunnermeier and Pedersen, 2009; Gromb and Vayanos, 2002) as well as limits-to-arbitrage models (e.g. Kyle and Xiong, 2001). The term ϵ_t denotes the innovation term, which is a non-negative random variable whose density is Gamma with a unit mean and variance equal to $\frac{1}{\vartheta}$. A sufficient condition for positivity of the conditional mean, μ_t, is that all coefficients in (14) are positive, while imposing $\alpha_d + \alpha_w + \alpha_m + \gamma/2 < 1$ ensures stationarity. Estimations are carried out using the maximum likelihood (ML), and we impose

[17] Appendix B reports a complete description of various alternative MEM and linear specifications, as well as their estimates on the sample under investigation.

stationarity and positivity conditions upon estimating the models on the data.

Panel a)	**Estimation results**			
	Daily Amihud	*High-Low Amihud*	*Jump-robust Amihud*	*Realized Amihud*
ω	0.0160^a	0.0052^a	0.0030^a	0.0029^a
	(0.0022)	(0.0011)	(0.0007)	(0.0007)
α_d	0.0000	0.0000	0.1265^a	0.1358^a
	(0.0234)	(0.0227)	(0.0225)	(0.0225)
α_w	0.0011	0.3146^a	0.3808^a	0.3865^a
	(0.0494)	(0.0476)	(0.0401)	(0.0396)
α_m	0.6595^a	0.5549^a	0.4087^a	0.3983^a
	(0.0661)	(0.0466)	(0.0381)	(0.0373)
γ	0.0297	0.0546^a	0.0399^a	0.0371^a
	(0.0235)	(0.0103)	(0.0071)	(0.0069)
ϑ	1.4608^a	12.0371^a	24.7189^a	26.5139^a
	(0.0361)	(0.3188)	(0.5895)	(0.5591)
Panel b)	**Ljung-Box statistics (p–value)**			
LB(1)	0.0045	0.2788	0.6561	0.7265
LB(5)	0.0453	0.0213	0.1608	0.2813
LB(10)	0.0714	0.0980	0.0001	0.0000

Table 6: MEM-AHAR estimated coefficients with robust standard errors (in parenthesis). The bottom panel reports the p-value of the Ljung-Box statistics. Superscript *a, b* and *c* denote the 1%, 5%, and 10% significance levels, respectively. Sample period: January 3, 2006 – June 29, 2018.

Table 6 reports the estimation results of the MEM-AHAR model on the daily Amihud, high–low Amihud, and on the realized Amihud based on 5-minute returns (including the jump-robust version). Focusing on the last column of Panel a), the coefficients governing the dynamics of μ_t for the realized Amihud are all positive and strongly significant at a 1% significance level, with a value of persistence around 93.6%, as measured by $\hat{\alpha}_d + \hat{\alpha}_w + \hat{\alpha}_m + \hat{\gamma}/2$. In the HAR framework, the coefficients α_d, α_w and α_m summarize the trade impact at different timeframes, here induced by heterogeneity among market participants on market illiquidity. The estimated coefficients indicate that today's illiquidity is predicted by that of yesterday, the previous week and month with a greater influence of the latter two. This heterogeneous persistence of illiquidity is a novel result that could have asset pricing implications. The results do not change when adopting the jump-robust realized Amihud.

On the other hand, when noisier proxies of illiquidity are employed, such as in the daily Amihud or the high–low Amihud, the parameter associated with daily past illiquidity, α_d, is estimated on the lower bound, while the parameter α_w is significant only for the high–low Amihud. The only significant parameter is α_m, indicating that a substantial smoothing is required on the daily Amihud to disentangle the expected illiquidity signal from its noisy ex-post measurement. Analogous evidence is found in the volatility literature when employing the realized GARCH model of Hansen et al. (2012) instead of the classic GARCH model on squared returns. In other words, the model assigns a small

weight to the innovation term when the latter contains a substantial degree of measurement error. Furthermore, the implied persistence obtained by the estimates of the MEM-AHAR coefficients on the daily and high-low Amihud is 67.5% and 89.7%, respectively. These values are much lower than those obtained on the realized Amihud, which is in line with the evidence of the ACFs reported in Figure 5. Finally, the estimate of ϑ (which is reciprocal of the variance of ε) for the daily Amihud is found to be around 16 times smaller than that of the realized Amihud. This implies that the variability of the innovation term is 16 times larger when employing the daily Amihud rather than the realized Amihud. This proportion is drastically reduced (approximately to half) when employing the high–low Amihud.

Overall, the results presented in Table 6 remain valid, even when alternative model specifications are employed; for more, see Tables 9 and 10 in Appendix B. In particular, the distribution of the innovation term seems to be well described by a Gamma distribution, while more sophisticated distributional choices do not provide a remarkable improve in the fit.[18] This is due to the fact that the realized Amihud does not display extreme distributional features because the ratio between volatility and volume drastically reduces the observed kurtosis (see Table 5). Finally, Panel b) of Table 6 reports the p-value for the Ljung-Box statistics. All model specifications correctly capture the persistent features of the series at hand because of the HAR-type specification for μ_t; for instance, see Caporin et al. (2016, 2017).

5.1.3 Illiquidity and Stock Market Excess Returns

The economic rationale for analyzing the relationship between returns and illiquidity is twofold. First, higher expected market illiquidity leads to higher ex ante asset (excess) return. Second, as illustrate in Figure 5 and captured by the clustering illiquidity effect, illiquidity shocks are very persistent. Therefore, an illiquidity shock that happens now will raise expected illiquidity for the future, which in turn causes ex ante asset returns to rise and asset prices to fall.[19] Taken together, these mechanisms point to two hypotheses to be tested: a positive coefficient relating *expected* illiquidity and asset return; a negative one relating *unexpected* illiquidity and contemporaneous asset return. Following Amihud (2002), we carry out an analysis on the impact of illiquidity on stock market excess returns but here enhanced by more accurate estimates of realized illiquidity. The realized Amihud can be disentangled into two components: the *expected* illiquidity, as measured by the estimated conditional mean of the MEM-AHAR model, $\hat{\mu}_t$, and the *unexpected illiquidity*, as measured by the residual component $\hat{\varepsilon}_t$.

Table 7 reports the results of a simple regression analysis of the stock market excess returns (as measured by the difference between the returns of SPY and the risk free rate the U.S. 3-month treasury bills in our case) on illiquidity, that is

$$r_t^e = \beta_0 + \beta_1 \mathcal{A}_t + u_t,$$

[18] Figure 9 in the Appendix reports the probability-integral transform based on various MEM model specifications (including the mixture MEM of Caporin et al., 2017 presented in Appendix B.1). Even the simple MEM specifications with Gamma distributed innovations display a remarkable fit of the empirical distribution.

[19] Concerning stocks, this assumes that corporate cash flows are unaffected by market illiquidity.

or on its components

$$r_t^e = \beta_0 + \beta_1 \hat{\mu}_t + \beta_2 \hat{\epsilon}_t + u_t.$$

Panel a)	Total Illiquidity								
	Daily Amihud			*High–Low Amihud*			*Realized Amihud*		
	daily	weekly	monthly	daily	weekly	monthly	daily	weekly	monthly
Constant	0.0363	0.0644	0.1515^a	0.0853	0.1016^c	0.1411^b	0.1747^a	0.1055^b	0.1337^a
	(0.0359)	(0.0436)	(0.0492)	(0.0605)	(0.0530)	(0.0579)	(0.0489)	(0.0511)	(0.0510)
Illiquidity	-0.6747	-1.2443	-3.0133^a	-1.6627	-1.9886^c	-2.7879^b	-3.6736^a	-2.1905^c	-2.7951^b
	(0.9147)	(1.0050)	(1.1137)	(1.3896)	(1.1566)	(1.2980)	(1.0687)	(1.1414)	(1.2282)
	Diagnostic								
R^2	0.0007	0.0044	0.0533	0.0011	0.0056	0.0341	0.0034	0.0056	0.0314
R^2 adj.	0.0004	0.0028	0.0464	0.0008	0.0040	0.0271	0.0031	0.0040	0.0243
F-test (p-value)	0.2628	0.1865	0.0106	0.1195	0.1169	0.0521	0.0020	0.1165	0.0657
Panel b)	Illiquidity decomposition								
	Daily Amihud			*High–Low Amihud*			*Realized Amihud*		
Constant	-0.0334	0.061	-0.0184	-0.0373	0.0471	0.0285	-0.0731	-0.0529	-0.1612^c
	(0.0877)	(0.0653)	(0.0720)	(0.0726)	(0.0550)	(0.0577)	(0.0710)	(0.0598)	(0.0917)
Expected Illiquidity	0.7428	-1.1749	0.4537	0.8171	-0.8852	-0.4951	1.66	1.241	3.6338^c
	(1.8686)	(1.3687)	(1.5292)	(1.5508)	(1.1404)	(1.2079)	(1.6072)	(1.2600)	(1.8563)
Unexpected Illiquidity	-0.786	-1.274	-7.9535^a	-3.1602^c	-4.6013^c	-17.0426^a	-10.2752^a	-14.0262^a	-37.7907^a
	(0.9224)	(1.1798)	(2.5456)	(1.7577)	(2.5736)	(6.0024)	(1.8958)	(5.0226)	(13.5283)
	Diagnostic								
R^2	0.0010	0.0044	0.0821	0.0025	0.0084	0.0748	0.0107	0.0254	0.1619
R^2 adj.	0.0003	0.0012	0.0687	0.0019	0.0052	0.0613	0.0101	0.0223	0.1496
F-test (p-value)	0.6132	0.6884	0.0076	0.0536	0.2004	0.0132	0.0000	0.0010	0.0000

Table 7: Analysis regressing stock market excess returns on illiquidity measures (the top of the table) and on illiquidity decomposed into exepcted and unexpected components (the bottom of the table). The coefficients and Newey and West (1987) robust standard errors (in parenthesis) are multiplied by 100. Superscript *a*, *b* and *c* denote the 1%, 5%, and 10% levels of significance, respectively.

In Panel a), when employing the realized Amihud as the explanatory variable, the estimate of β_1 suggests that illiquidity is in a significantly negative relationship with the excess return. This holds true when aggregating at weekly and monthly (nonoverlapping) horizons. Notably, the R^2 turns out to be particularly large at the monthly horizon, being above 16%. Contrary to this, the relationship is less pronounced when employing the classic daily Amihud as the regressor. In particular, β_1 is not significant at the daily and weekly frequencies, but it is significant when the aggregation at monthly level is considered (in this case, the R^2 is around 5%). Again, this signals the fact that a less accurate measurement of illiquidity obtained via the daily Amihud masks the fundamental relationship between returns and illiquidity.

The results most closely related to testing the hypotheses discussed above are shown in Panel b) of Table 7. The estimated coefficients support the two hypotheses. Although not statistically significant, expected illiquidity is positively related to asset return. On the contrary, unexpected illiquidity is negatively and significantly associated with asset return. More specifically, the expected illiquidity weighs positively on returns but it is never significant at the daily and weekly frequencies

(irrespective of the measure adopted), while the *unexpected* illiquidity (as measured by the residuals of the MEM-AHAR model) is significantly and negatively related with the excess returns when both the realized illiquidity measures (i.e. the realized and high–low Amihud metrics) are employed. Instead, the unexpected liquidity for the classic daily Amihud is only significant at the monthly horizon. This result squares well with the idea that the residual term of the MEM-AHAR model estimated on the daily Amihud is made of two components: the prediction error and the measurement error, where the latter seems to dominate at the daily and weekly frequencies.

5.2 Currency Market Illiquidity

Another way to assess the general validity of the realized illiquidity and its higher accuracy in measuring high-frequency market liquidity is by considering another financial instrument and using a meaningful episode, which is a sort of natural experiment. Through the lenses of the theory developed in Section 2, the announcement of the cap removal of the Swiss franc by the Swiss National Bank (SNB) on January 15, 2015, represents an ideal framework for conducting further testing. Starting from September 6, 2011, the SNB set a minimum exchange rate of 1.20 francs to the euro (capping the franc's appreciation), stating that "the value of the franc is a threat to the economy" and that it was "prepared to buy foreign currency in unlimited quantities." This means that the SNB had a declared binding *cap* on the transaction price that was removed on January 15, 2015.

In terms of the trading model presented in Section 2, the SNB can be considered the special $(J+1)$-th trader. The SNB intervention strategy of selling CHF for EUR in potentially unlimited quantities would be implemented if the average of the reservation prices of the remaining J traders ever fell below the cap, that is if $\frac{1}{J}\sum_{j=1}^{J} p_{i,j}^{*} < \log(1.2)$.[20] Indeed, despite the cap on the transaction price, the reservation prices of individual traders might well be below the 1.20 threshold. For instance, a trader with a reservation price of 1.12 (as the agents with the actual lowest forecast in Thomson Reuters survey before the SNB cap removal) is inclined to sell EUR for CHF. In other words, the SNB buys (sells) foreign (domestic) currency to guarantee that the transaction price is above the threshold, that is

$$p_i^{EUR|CHF} = \frac{1}{J+1}\sum_{j=1}^{J+1} p_{i,j}^{EUR|CHF,*} \geq \log(1.2), \tag{15}$$

where $p_{i,J+1}^{EUR|CHF,*} = \left(\log(1.2) - \frac{1}{J}\sum_{j=1}^{J} p_{i,j}^{EUR|CHF,*}\right) \times \mathbb{I}\left(\sum_{j=1}^{J} p_{i,j}^{EUR|CHF,*} < \log(1.2)\right)$, and $\mathbb{I}(\cdot)$ is the indicator function. The enforcement of the capping regime by the SNB generates extra trading volume. In particular, the trading volume is as follows

$$v_i^{EUR|CHF} = \frac{\ell_i}{2}\sum_{j=1}^{J} |\Delta p_{i,j}^{EUR|CHF,*} - \frac{1}{J}\sum_{j=1}^{J} \Delta p_{i,j}^{EUR|CHF,*}| + v_i^{SNB}, \tag{16}$$

where v_i^{SNB} is the trading volume generated by the central bank to maintain the cap on the FX rate. Hence, the model prescribes a low volatility of the observed returns because of the implicit constraint

[20] See Breedon et al. (2022) for a discussion of how the SNB surprised the market and how it actually implemented the intervention strategy by setting a huge ask volume at 1.20. Furthermore, the Thomson Reuters survey indicates a wide dispersion of the beliefs of professional market participants around 1.20 for most of the capping period.

given by the capping and a larger volume because of the SNB interventions. This implies that the realized illiquidity is lower (higher) before (after) the removal of the FX capping regime.

To empirically explore these model implications, we analyze at the daily time series of realized Amihud of the EUR/CHF and the USD/CHF FX spot rates covering the period November 1, 2011, to September 30, 2021. The time series are constructed from two distinct data sets. First, the CLS Group — the largest payment system for the settlement of foreign exchange transactions — provides us hourly data on the traded volume representative for the FX global activity on both the EUR/CHF and USD/CHF rates.[21] Second, 1-minute EUR/CHF and USD/CHF spot rates (bid, ask, high, low, and mid-quotes) are obtained from Olsen Financial Technologies. Given that trading on FX rates is active 24 hours a day but concentrated during the so-called London hours (Ranaldo and Somogyi, 2021), we consider the intra-daily returns and volume solely between 8 a.m. and 8 p.m. (GMT time), thus limiting the influence of possible noisy observations associated with overnight hours in which there is minimal trading activity. Our final data set consists of 1, 943, 760 intra-daily 1-minute returns and 32, 396 hourly trading volume for a total of 2, 492 trading days. Once again, we consider the returns sampled at both 5-minute frequencies to compute RPV and RPV_C, while the daily volume is computed simply by aggregating the hourly volume.

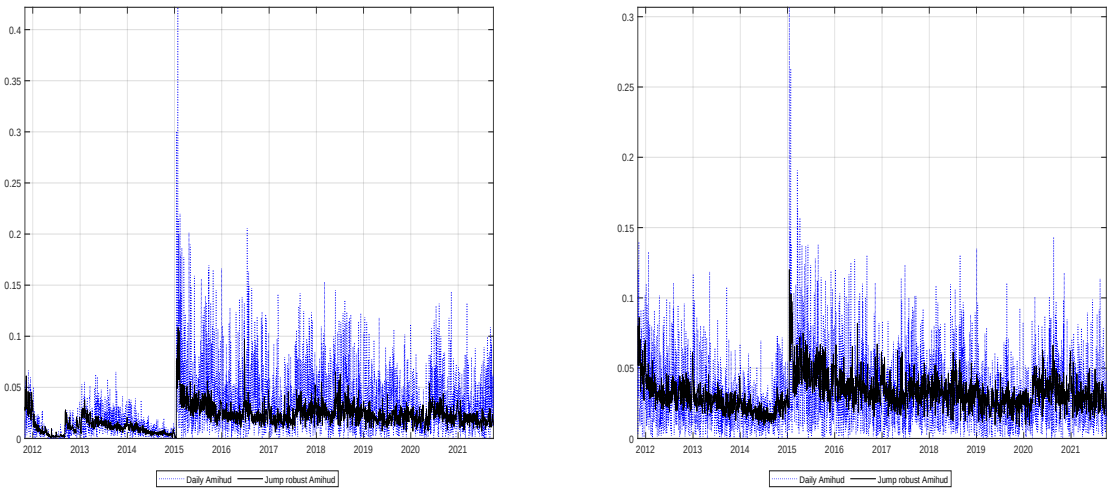

(a) EUR/CHF (b) USD/CHF

Figure 7: Daily Amihud (blue dotted lines, see Amihud (2002)) vs. the realized Amihud (black solid lines) of EUR/USD (Panel a) and USD/CHF (Panel b) exchange rates. Sample period: November 1, 2011 – September 30, 2021. Both series are scaled by a factor of E+11.

Figure 7 displays the time series of the realized Amihud (black solid lines) and daily Amihud (blue dashed lines) of the EUR/USD (Panel a) and USD/CHF (Panel b) rates. As for SPY, the illiquidity clustering phenomenon is evident. High illiquidity characterizes the years after the onset of the sovereign debt crisis (in the period between 2010 and 2012). This period of stress greatly characterized the Swiss franc being considered a safe haven currency and giving it strong appreciation pressures (Jordan, 2020). On January 15, 2015, after the announcement by the SNB, we observe the highest peak

[21] See Ranaldo and Somogyi (2021) and Cespa et al. (2021) for a discussion and empirical evidence on the global representativeness of CLS data.

of illiquidity, which remains very high for several months after this event. For both rates, Figure 7 reconfirms that the classic daily Amihud is much noisier than the corresponding realized version.

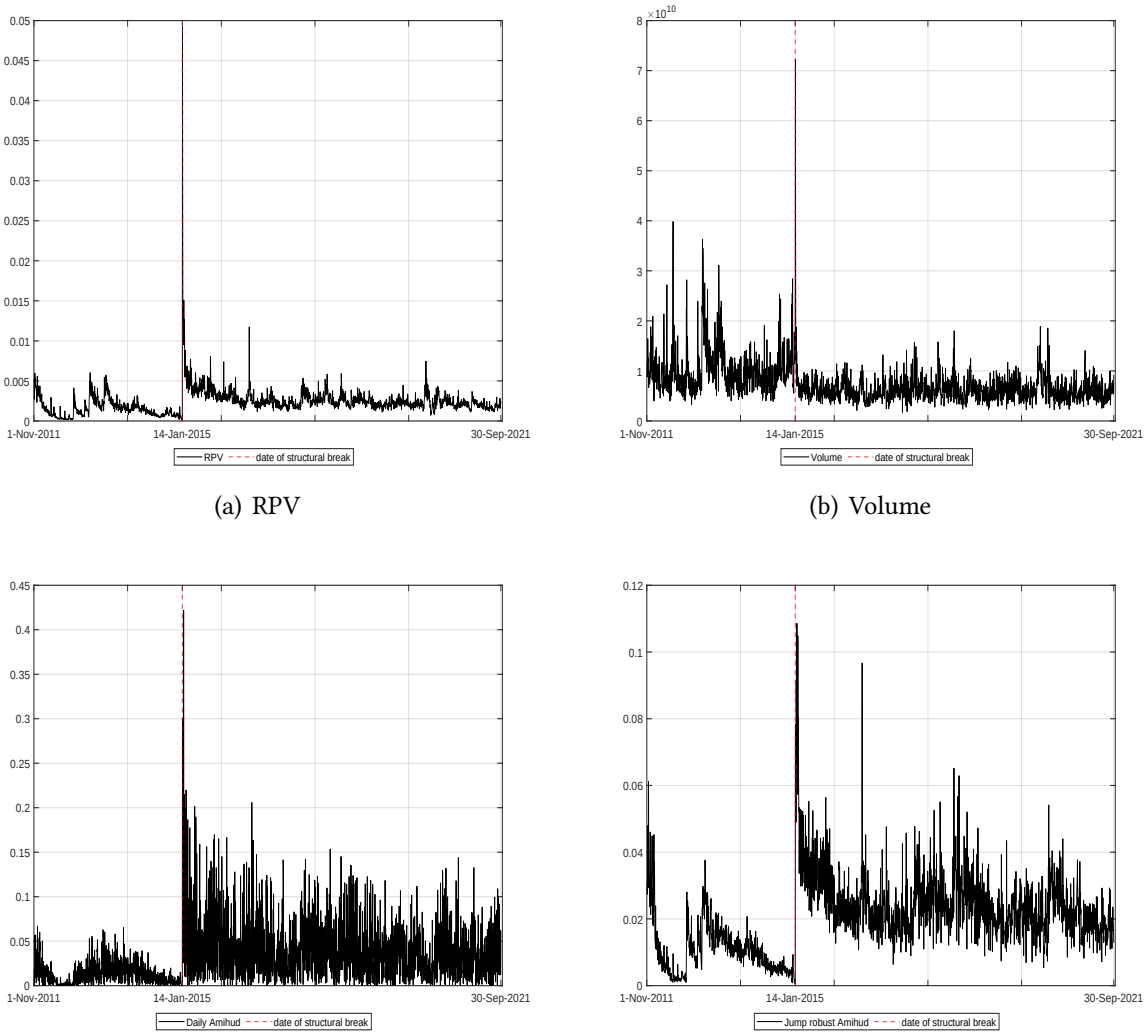

(a) RPV (b) Volume

(c) Daily Amihud (d) Realized Amihud

Figure 8: Break dates. The figures report the time series of RPV, volume, daily Amihud, and realized Amihud for the EUR/CHF rate (black solid line). The red vertical line denotes the break date, which is estimated by means of the Bai and Perron (1998) test for unknown break points. The test is performed with 15% trimming at the beginning and the end of the sample period and between break dates.

Figure 8 reports the result of Bai and Perron (1998)'s testing procedure to identify the date of a level break (if any) in a time series of RPV, volume, daily Amihud, and realized Amihud of EUR/CHF. The test considers the possible presence of one or more structural changes occurring at unknown dates: in particular, Bai and Perron (1998) propose a procedure designed to estimate the break dates, while testing for the presence of structural changes at the same time. We apply the Bai and Perron (1998) test with 15% trimming at the beginning and the end of the sample period and between the break dates (see also Casini and Perron, 2019, for a review and up-to-date recommendations about the procedure).[22] The series are characterized by strong persistence, and the procedure of Bai and Perron (1998) is robust to autocorrelation and heteroskedasticity. In all cases, the test identifies a

[22]We are grateful to Alessandro Casini for having shared with us the MATLAB codes for the break test.

significant break date on January 14, 2015, thus suggesting that the level of the series changes before and after this break date. The results for USD/CHF are reported in the Appendix and are analogous to those reported for EUR/CHF. In addition to significantly impacting a single currency pair, this result suggests that important events such as currency regime changes can affect commonality in the liquidity of financial securities.

	Estimation Results							
	EUR/CHF				USD/CHF			
	Realized Amihud	*RPV*	*Volume*	*Daily Amihud*	*Realized Amihud*	*RPV*	*Volume*	*Daily Amihud*
$Mean_1$	0.0109^a	0.0016^a	1.0159^a	0.0129^a	0.0279^a	0.0039^a	1.4617^a	0.0300^a
	(0.0015)	(0.0002)	(0.0390)	(0.0008)	(0.0013)	(0.0002)	(0.0384)	(0.0010)
$Mean_2$	0.0248^a	0.0027^a	0.6205^a	0.0422^a	0.0345^a	0.0038^a	1.1315^a	0.0352^a
	(0.0008)	(0.0001)	(0.0120)	(0.0010)	(0.0008)	(0.0001)	(0.0153)	(0.0007)
	Diagnostic							
R^2	0.3127	0.1009	0.2168	0.1638	0.0714	0.0004	0.1112	0.0076
D-W statistics	0.6384	0.6558	1.0136	1.7513	0.7912	0.9394	1.2655	1.8778

Table 8: Level estimation (robust standard errors in parenthesis) before and after the date January 14, 2015, for the EUR/CHF and USD/CHF FX rates. Superscripts *a*, *b*, and *c* denote the 1%, 5%, and 10% levels of significance, respectively. To account for heteroskedasticity and autocorrelation, the standard errors are computed based on the HAC estimator by following the automatic method in Andrews (1991) for the selection of the number of lagged autocovariances. Sample period: November 1, 2011 – September 30, 2021.

Table 8 reports the estimates of the mean of the series under investigation before and after the break date, which has been found on January 14, 2015. The results reported in the table strongly support the prescriptions of the theory. More specifically, the level of volatility (volume) significantly increases (decreases), thus leading to an increase of illiquidity (as measured by both daily and realized Amihud) on EUR/CHF. In a similar way, this shock also affects the other currency pair USD/CHF, which was not directly exposed to the capping on the EUR/CHF rate.

6 Conclusion

Liquidity is crucial to the well-functioning of financial markets and depends on how trading volume impacts asset prices. Building on the simple trading mechanism introduced by Tauchen and Pitts (1983), we develop the theory of realized volatility in the context of measuring market liquidity. Similar to the spot volatility, the instantaneous liquidity, $\ell(t)$, is assumed to vary over time based on a dynamic process in continuous time; that is, liquidity is stochastic. We propose two realized illiquidity measures that we call *realized Amihud* and *high-low Amihud*. The former is defined as the ratio between the realized power variation computed using intraday data and trading volume while the latter is the ratio between the high-low range based on daily data and volume. We demonstrate theoretically and numerically that the realized Amihud is a very accurate measure and that both realized illiquidity metrics refine the widely used measure of volume price impact proposed in Amihud (2002). Furthermore, by employing the theory of multipower variation in Barndorff-Nielsen and Shephard (2003, 2004, 2006) we develop a simple theory for jumps that capture the information component of market illiquidity.

Five main results stand out from our econometric analysis based on more than a decade of representative data for the stock and currency markets. First, the realized Amihud provides a very precise measurement of the inverse of integrated liquidity, namely the integral $\mathcal{L} = \int_0^1 \ell(s)ds$, over periods of fixed length (e.g., a day, a week, or a month). If intraday data are not accessible, then the high-low Amihud ensures a more precise illiquidity measurement than the classic daily Amihud proxy. Second, the proposed test statistic is effective in detecting significant information jumps – that is – illiquidity reaction to impactful news common to all traders. Based on this, we also propose a jump-robust version of the realized illiquidity estimator. Third, using heterogeneous autoregressive specifications (HAR) and multiplicative error models (MEM) we show that illiquidity is highly and heterogeneously persistence in the sense that an illiquidity shock triggers prolonged effects and today's illiquidity is predicted by that of yesterday, of one week and one month ago. Fourth, illiquidity undergoes leverage effects in the sense that it increases more in market downturns and illiquidity shocks materialize and are more persistent when associated with negative returns. Finally, we find that it is rather the unexpected part of illiquidity that negatively predicts returns consistent with the idea that the persistent effect of an illiquidity shock increases expected future illiquidity thus decreasing asset prices.

Prior research used the traditional Amihud measure in asset pricing (among the most recent papers, see, e.g., Lou and Shu, 2017 and Amihud and Noh, 2021). In this paper, we have proposed more accurate measures of realized illiquidity and we have highlighted their characteristics such as (illiquidity) jumps, heterogeneous clustering, and leverage effects. We have demonstrated that all this helps explain the temporal variation in asset returns. Future research should highlight whether and how these features predict the cross-section of asset prices and can apply what we have proposed on many other aspects of financial economics.

References

Abdi, F. and Ranaldo, A. (2017). A simple estimation of bid-ask spreads from daily close, high, and low prices. *The Review of Financial Studies*, 30(12):4437–4480.

Aït-Sahalia, Y. and Jacod, J. (2014). High-frequency financial econometrics. In *High-Frequency Financial Econometrics*. Princeton University Press.

Amihud, Y. (2002). Illiquidity and stock returns: Cross-section and time-series effects. *Journal of Financial Markets*, 5:31–56.

Amihud, Y. and Mendelson, H. (1986). Asset pricing and the bid-ask spread. *Journal of Financial Economics*, 17:223–249.

Amihud, Y. and Noh, J. (2021). Illiquidity and stock returns II: Cross-section and time-series effects. *The Review of Financial Studies*, 34(4):2101–2123.

Andersen, T. G. (1996). Return volatility and trading volume: An information flow interpretation of stochastic volatility. *The Journal of Finance*, 51(1):169–204.

Andersen, T. G. and Bollerslev, T. (1998). Answering the skeptics: Yes, standard volatility models do provide accurate forecasts. *International Economic Review*, 39(4):885–905.

Andersen, T. G., Bollerslev, T., Diebold, F. X., and Vega, C. (2007). Real-time price discovery in global stock, bond and foreign exchange markets. *Journal of International Economics*, 73(2):251–277.

Andrews, D. W. (1991). Heteroskedasticity and autocorrelation consistent covariance matrix estimation. *Econometrica: Journal of the Econometric Society*, 59:817–858.

Bai, J. and Perron, P. (1998). Estimating and testing linear models with multiple structural changes. *Econometrica: Journal of the Econometric Society*, 66:47–78.

Bandi, F. M., Kolokolov, A., Pirino, D., and Renò, R. (2020). Zeros. *Management Science*, 66(8):3466–3479.

Bandi, F. M. and Russell, J. R. (2008). Microstructure noise, realized variance, and optimal sampling. *The Review of Economic Studies*, 75(2):339–369.

Barndorff-Nielsen, O. E., Hansen, P. R., Lunde, A., and Shephard, N. (2008). Designing realized kernels to measure the ex post variation of equity prices in the presence of noise. *Econometrica: Journal of the Econometric Society*, 76(6):1481–1536.

Barndorff-Nielsen, O. E. and Shephard, N. (2002a). Econometric analysis of realized volatility and its use in estimating stochastic volatility models. *Journal of the Royal Statistical Society Series B*, 64:253–280.

Barndorff-Nielsen, O. E. and Shephard, N. (2002b). Estimating quadratic variation using realized variance. *Journal of Applied Econometrics*, 17(5):457–477.

Barndorff-Nielsen, O. E. and Shephard, N. (2003). Realized power variation and stochastic volatility models. *Bernoulli*, 9(2):243–265.

Barndorff-Nielsen, O. E. and Shephard, N. (2004). Power and bipower variation with stochastic volatility and jumps. *Journal of Financial Econometrics*, 2(1):1–37.

Barndorff-Nielsen, O. E. and Shephard, N. (2006). Econometrics of testing for jumps in financial economics using bipower variation. *Journal of Financial Econometrics*, 4(1):1–30.

Bauwens, L., Hafner, C. M., and Laurent, S. (2012). *Handbook of volatility models and their applications*, volume 3. John Wiley & Sons.

Bollerslev, T., Li, J., Xue, Y., et al. (2018). Volume, volatility and public news announcements. *The Review of Economic Studies*, 85(4):2005–2041.

Breedon, F., Chen, L., Ranaldo, A., and Vause, N. (2022). Judgement day: Algorithmic trading around the swiss franc cap removal. *Journal of International Economics*, (forthcoming).

Brunnermeier, M. K. and Pedersen, L. H. (2009). Market liquidity and funding liquidity. *The Review of Financial Studies*, 22:2201–2238.

Caporin, M., Rossi, E., and Santucci de Magistris, P. (2016). Volatility jumps and their economic determinants. *Journal of Financial Econometrics*, 14(1):29–80.

Caporin, M., Rossi, E., and Santucci de Magistris, P. (2017). Chasing volatility: A persistent multiplicative error model with jumps. *Journal of Econometrics*, 198(1):122–145.

Casini, A. and Perron, P. (2019). Structural breaks in time series. Oxford University Press.

Catania, L. (2020). The leverage effect and propagation. *SSRN*.

Cespa, G., Gargano, A., Riddiough, S. J., and Sarno, L. (2021). Foreign exchange volume. *The Review of Financial Studies*, 35(5):2386–2427.

Chaboud, A. P., Chernenko, S. V., and Wright, J. H. (2008). Trading activity and macroeconomic announcements in high-frequency exchange rate data. *Journal of the European Economic Association*, 6(2-3):589–596.

Chan, W. H. and Maheu, J. M. (2002). Conditional jump dynamics in stock market returns. *Journal of Business & Economic Statistics*, 20(3):377–389.

Christensen, K., Oomen, R. C., and Renò, R. (2022). The drift burst hypothesis. *Journal of Econometrics*, 227:461–497.

Clark, P. (1973). A subordinated stochastic process model with finite variance for speculative prices. *Econometrica: Journal of the Econometric Society*, 41(1):135–55.

Collin-Dufresne, P. and Fos, V. (2016). Insider trading, stochastic liquidity, and equilibrium prices. *Econometrica: Journal of the Econometric Society*, 84(4):1441–1475.

Comte, F. and Renault, E. (1998). Long memory in continuous-time stochastic volatility models. *Mathematical Finance*, 8(4):291–323.

Corsi, F. (2009). A simple approximate long-memory model of realized volatility. *Journal of Financial Econometrics*, 7:174–196.

Corwin, S. A. and Schultz, P. H. (2012). A simple way to estimate bid-ask spreads from daily high and low prices. *The Journal of Finance*, 67:719–759.

Cox, J. C., Ingersoll, J. E., and Ross, S. A. (2005). A theory of the term structure of interest rates. In *Theory of Valuation*. World Scientific.

Dubofsky, D. A. and Groth, J. C. (1984). Exchange listing and stock liquidity. *Journal of Financial Research*, 7:291–302.

Engle, R. (2002). New frontiers for ARCH models. *Journal of Applied Econometrics*, 17(5):425–446.

Engle, R. F. and Gallo, G. M. (2006). A multiple indicators model for volatility using intra-daily data. *Journal of Econometrics*, 131(1-2):3–27.

Epps, T. W. and Epps, M. L. (1976). The stochastic dependence of security price changes and transaction volumes: Implications for the mixture-of-distributions hypothesis. *Econometrica: Journal of the Econometric Society*, 44:305–321.

Fong, K. Y. L., Holden, C. W., and Tobek, O. (2018). Are volatility over volume liquidity proxies useful for global or us research? Kelley School of Business Research Paper No. 17-49.

Foucault, T., Pagano, M., and Röell, A. (2013). *Market Liquidity: Theory, Evidence, and Policy*. Oxford University Press.

Glosten, L. R., Jagannathan, R., and Runkle, D. E. (1993). On the relation between the expected value and the volatility of the nominal excess return on stocks. *The Journal of Finance*, 48(5):1779–1801.

Gromb, D. and Vayanos, D. (2002). Equilibrium and welfare in markets with financially constrained arbitrageurs. *Journal of Financial Economics*, 66(2-3):361–407.

Grossman, S. J. and Miller, M. H. (1988). Liquidity and market structure. *The Journal of Finance*, 43(3):617–633.

Hameed, A., Kang, W., and Viswanathan, S. (2010). Stock market declines and liquidity. *The Journal of Finance*, 65(1):257–293.

Hansen, P. R., Huang, Z., and Shek, H. H. (2012). Realized GARCH: a joint model for returns and realized measures of volatility. *Journal of Applied Econometrics*, 27(6):877–906.

Hasbrouck, J. (2009). Trading costs and returns for us equities: Estimating effective costs from daily data. *The Journal of Finance*, 64(3):1445–1477.

Heston, S. L. (1993). A closed-form solution for options with stochastic volatility with applications to bond and currency options. *The Review of Financial Studies*, 6(2):327–343.

Hurvich, C. M., Moulines, E., and Soulier, P. (2005). Estimating long memory in volatility. *Econometrica: Journal of the Econometric Society*, 73(4):1283–1328.

Hurvich, C. M. and Ray, B. K. (2003). The local Whittle estimator of long-memory stochastic volatility. *Journal of Financial Econometrics*, 1(3):445–470.

Jiang, G. J., Lo, I., and Verdelhan, A. (2011). Information shocks, liquidity shocks, jumps, and price discovery: Evidence from the US treasury market. *Journal of Financial and Quantitative Analysis*, 46(2):527–551.

Jordan, T. (2020). Small country - big challenges: Switzerland's monetary policy response to the coronavirus pandemic. *2020 IMF Michel Camdessus Central Banking Lecture*.

Karpoff, J. M. (1987). The relation between price changes and trading volume: A survey. *Journal of Financial and Quantitative Analysis*, 22(1):109–126.

Keynes, J. M. (1936). *The General Theory of Employment, Interest, and Money*. Palgrave Macmillan.

Kolokolov, A. and Renò, R. (2021). Jumps or staleness? *Available at SSRN 3882775*.

Kyle, A. S. (1985). Continuous auctions and insider trading. *Econometrica: Journal of the Econometric Society*, 53:1315–1335.

Kyle, A. S. and Xiong, W. (2001). Contagion as a wealth effect. *The Journal of Finance*, 56:1401–1440.

Lee, S. S. (2011). Jumps and information flow in financial markets. *The Review of Financial Studies*, 25(2):439–479.

Liu, L. Y., Patton, A. J., and Sheppard, K. (2015). Does anything beat 5-minute RV? A comparison of realized measures across multiple asset classes. *Journal of Econometrics*, 187(1):293–311.

Lou, X. and Shu, T. (2017). Price impact or trading volume: Why is the Amihud (2002) measure priced? *The Review of Financial Studies*, 30(12):4481–4520.

Maheu, J. M. and McCurdy, T. H. (2004). News arrival, jump dynamics, and volatility components for individual stock returns. *The Journal of Finance*, 59(2):755–793.

Maheu, J. M., McCurdy, T. H., and Zhao, X. (2013). Do jumps contribute to the dynamics of the equity premium? *Journal of Financial Economics*, 110(2):457–477.

Müller, U., Dacorogna, M., Dav, D. A., Pictet, O., Olsen, R., and Ward, J. (1993). Fractals and intrinsic time – a challenge to econometricians. Working paper, Olsen and Associates.

Müller, U. A., Dacorogna, M. M., Davé, R. D., Olsen, R. B., Pictet, O. V., and Von Weizsäcker, J. E. (1997). Volatilities of different time resolutions-analyzing the dynamics of market components. *Journal of Empirical Finance*, 4(2-3):213–239.

Newey, W. K. and West, K. D. (1987). A simple, positive semi-definite, heteroskedasticity and autocorrelation consistent covariance matrix. *Econometrica: Journal of the Econometric Society*, 55:703–708.

Parkinson, M. (1980). The extreme value method for estimating the variance of the rate of return. *Journal of Business*, 53:61–65.

Perraudin, W. and Vitale, P. (1996). Interdealer trade and information flows in a decentralized foreign exchange market. In Jeffrey A. Frankel, G. G. and Giovannini, A., editors, *The Microstructure of Foreign Exchange Markets*. University of Chicago Press.

Podolskij, M. and Vetter, M. (2009). Bipower-type estimation in a noisy diffusion setting. *Stochastic Processes and their Applications*, 119(9):2803–2831.

Ranaldo, A. and Santucci de Magistris, P. (2022). Liquidity in the global currency market. *Journal of Financial Economics*, 146:859–883.

Ranaldo, A. and Somogyi, F. (2021). Asymmetric information risk in FX markets. *Journal of Financial Economics*, 140(2):391–411.

Roll, R. (1984). A simple implicit measure of the effective bid-ask spread in an efficient market. *The Journal of Finance*, 39:1127–1139.

Silber, W. L. (1975). Thinness in capital markets: The case of the tel aviv stock exchange. *Journal of Financial and Quantitative Analysis*, 10(1):129–142.

Tauchen, G. E. and Pitts, M. (1983). The price variability-volume relationship on speculative markets. *Econometrica: Journal of the Econometric Society*, 51:485–505.

Vasicek, O. (1977). An equilibrium characterization of the term structure. *Journal of financial economics*, 5(2):177–188.

White, H. (1980). A heteroskedasticity-consistent covariance matrix estimator and a direct test for heteroskedasticity. *Econometrica: Journal of the Econometric Society*, 48:817–838.

Zhang, L., Mykland, P. A., and Aït-Sahalia, Y. (2005). A tale of two time scales: Determining integrated volatility with noisy high-frequency data. *Journal of the American Statistical Association*, 100(472):1394–1411.

A Proofs

A.1 Proof of Proposition 1

The proof of Proposition 1 proceeds as follows. By the properties of the super-position of independent processes, the limit for $\delta \to 0$ (or $I \to \infty$) of RPV is as follows:

$$p \lim_{I\to\infty} \delta^{1/2} RPV = \sqrt{\frac{2}{\pi}}\mathcal{S}, \tag{17}$$

where $\mathcal{S} = \int_0^1 \overline{\sigma}(s)ds$ is the integrated average standard deviation and where the latter is defined as $\overline{\sigma}(t) = \frac{1}{J}\sqrt{\sum_{j=1}^{J}\sigma_j^2(t)}$. Indeed, similar to Barndorff-Nielsen and Shephard (2002b), $\Delta p_i = \frac{1}{J}\sum_{j=1}^{J}\Delta p_{i,j}^*$ is equivalent in law to $\int_{\delta(i-1)}^{\delta i}\overline{\sigma}(t)dW^*(t)$, where $\overline{\sigma}(t) = \frac{1}{J}\sqrt{\sum_{j=1}^{J}\sigma_j^2(t)}$. The aggregated volume on a unit (daily) interval is $v = \sum_{i=1}^{I} v_i$, and letting $I \to \infty$, we get

$$p \lim_{I\to\infty} \delta^{1/2} v = \frac{\mathcal{L}}{2}\sqrt{\frac{2}{\pi}}\overline{\mathcal{S}}, \tag{18}$$

with $\overline{\mathcal{S}} = \frac{1}{J}\sum_{j=1}^{J}\int_0^1 \varsigma_j(s)ds$, where $\varsigma_j(t) = \sqrt{(J-1)^2\sigma_j^2(t) + \sum_{s\neq j}\sigma_s^2(t)}$ and $\mathcal{L} = \int_0^1 \ell(s)ds$ denotes the *integrated liquidity*. Hence, we get

$$p \lim_{I\to\infty} \mathcal{A} = \frac{2\mathcal{S}}{\mathcal{L}\overline{\mathcal{S}}}, \tag{19}$$

which reflects the ratio of the total average standard deviation carried by each trader. If $J = 2$, then $\overline{\mathcal{S}} = 2\mathcal{S}$, so that equation (6) in Proposition 1 follows directly, that is, $p\lim_{I\to\infty}\mathcal{A} = \frac{1}{\mathcal{L}}$.

Furthermore, by straightforward application of Barndorff-Nielsen and Shephard (2003, p.260), we get

$$\frac{\log\left(\sqrt{\pi\delta/2}\cdot v\right) - \log\left(\mathcal{S}\mathcal{L}\right)}{\sqrt{\frac{\delta(\pi/2-1)RV}{(\pi\delta/2)RPV^2}}} \xrightarrow{d} N(0,1), \tag{20}$$

where RV is the realized variance and is defined as $RV^{=}\sum_{i=1}^{I}(r_i)^2$; for more, see, among others, Andersen and Bollerslev (1998). Following Barndorff-Nielsen and Shephard (2002a,b) and taking the limit for $\delta \to 0$ (i.e., $I \to \infty$), we get $p\lim_{I\to\infty} RV = \frac{1}{J^2}\mathcal{V}$, where $\mathcal{V} = \sum_{j=1}^{J}\mathcal{V}_j$ is the variation of the asset price on the unit interval generated by the aggregated individual components of r. The term $\mathcal{V}_j = \int_0^1 \sigma_j(s)^2 ds$ is the *integrated variance* associated with the j-th trader's specific component. By noticing that $\log(\mathcal{A}) = \log\left(\sqrt{\pi\delta/2}\cdot RPV\right) - \log\left(\sqrt{\pi\delta/2}\cdot v\right)$, the result in (7) follows. ■

A.2 Traders homogeneity

Analogous results are obtained if $J \geq 2$ assuming homogeneity of traders, that is, $\sigma_j = \sigma \quad \forall j = 1, 2, \ldots, J$. In particular, the following proposition highlights the main determinants of the realized Amihud as an illiquidity measure under homogeneity of traders when $J \geq 2$.

Proposition 2. *Consider the illiquidity measure defined in (5), the equilibrium relation in (1), and the diffusive process for reservation prices in (3). Assume that σ_j and $\ell(t)$ are strictly positive càdlàg processes with (almost surely) square integrable sample paths with $\sigma_j(t) = \sigma(t)\ \forall j = 1, \ldots, J$. As $I \to \infty$ (i.e., $\delta \to 0$)*

$$p \lim_{I\to\infty} \mathcal{A} = \frac{2}{J\sqrt{J-1}\mathcal{L}}, \tag{21}$$

Furthermore, as $I \to \infty$

$$\frac{\log(\mathcal{A}) - \log\left(\frac{2}{\mathcal{L}J\sqrt{(J-1)}}\right)}{\sqrt{\frac{J\delta(\pi/2-1)RV}{(J-1)(\pi\delta/2)RPV^2}}} \xrightarrow{d} N(0,1), \tag{22}$$

where $RV^{=} \sum_{i=1}^{I} (r_i)^2$ is the realized variance.

The proof of Proposition 2 follows the same steps as the proof of Proposition 1 in Section A.1. In this case, $\overline{S} = J\sqrt{J-1}\mathcal{S}$, so that

$$p \lim_{I\to\infty} \mathcal{A} = \frac{2}{J\sqrt{J-1}\mathcal{L}}. \tag{23}$$

In this case, it follows that in the limit for $I \to \infty$, the realized Amihud is inversely proportional to the integrated illiquidity and to the number of active traders in the market. By relaxing the assumption of homogeneity, $\mathcal{A}$ would converge in probability to the integrated illiquidity times the ratio of two measures of integrated volatility, namely $\frac{2\mathcal{S}}{\overline{S}}$, that is, a weighted average of the price variability carried by each trader. Furthermore,

$$\frac{\log\left(\sqrt{\pi\delta/2}\cdot v\right) - \log\left(\mathcal{S}J\sqrt{J-1}\mathcal{L}\right)}{\sqrt{\frac{\delta(\pi/2-1)RV}{((J-1)\pi\delta/2)RPV^2}}} \xrightarrow{d} N(0,1), \tag{24}$$

so that

$$\frac{\log(\mathcal{A}) - \log\left(\frac{2}{\mathcal{L}J\sqrt{(J-1)}}\right)}{\sqrt{\frac{J\delta(\pi/2-1)RV}{(J-1)(\pi\delta/2)RPV^2}}} \xrightarrow{d} N(0,1). \tag{25}$$

■

B Modeling Realized Amihud

In this section, we propose an econometric specification to characterize the dynamic evolution and distributional features of the realized Amihud. First, we consider parametric models belonging to the class of multiplicative error models (MEM), as introduced by Engle (2002) and Engle and Gallo (2006).

B.1 A mixture MEM model

Following the same approach adopted by Caporin et al. (2017), it is possible to construct a MEM model featuring a component responsible for generating large and unexpected moves in illiquidity. In particular, following Caporin et al. (2017), we model $\mathcal{A}$ according to an AMEM with a mixture specification, namely AMEM-Mix. In the AMEM-Mix, $\mathcal{A}_t$ is given by the product of three elements:

$$\mathcal{A}_t = \mu_t Z_t \epsilon_t, \tag{26}$$

where μ_t is the conditional mean, and it follows asymmetric MEM (AMEM) dynamics:

$$\mu_t = \omega + \alpha \mathcal{A}_{t-1} + \beta \mu_{t-1} + \gamma D_{t-1} \mathcal{A}_{t-1}, \tag{27}$$

where D_{t-1} is a dummy variable taking a value of 1 if the return is negative and 0 otherwise; it accounts for an asymmetric response of illiquidity to good or bad news. The term ϵ_t denotes the innovation term, whose density (conditional on the information set $\mathcal{F}_{t-1}$) is

$$f(\epsilon_t|\mathcal{F}_{t-1}) = \frac{1}{\Gamma(\vartheta)} \vartheta^{\vartheta} \epsilon_t^{\vartheta-1} e^{-\vartheta \epsilon_t}, \qquad \epsilon_t > 0, \quad \vartheta > 0. \tag{28}$$

This means that $\epsilon_t|\mathcal{F}_{t-1}$ is a gamma-distributed random variable with unit mean and variance equal to $\frac{1}{\vartheta}$. Finally, the mixing term, Z_t, is assumed to be independent of ϵ_t and distributed as a compound Poisson random variable

$$Z_t = \begin{cases} d_\kappa & N_t = 0, \\ \sum_{j=1}^{N_t} Y_{j,t} & N_t > 0, \end{cases} \tag{29}$$

where the expected number of arrivals at time t (N_t) is governed by a Poisson random variable with a time-varying intensity, κ_t, and d_κ is a positive function of κ_t such that $E[Z_t \epsilon_t|\mathcal{F}_{t-1}] = 1$ and $E(\mathcal{A}|\mathcal{F}_{t-1}) = \mu_t$. Furthermore, $Y_{j,t}|\mathcal{F}_{t-1} \sim \Gamma(d_\kappa, \zeta)$. By the Poisson distribution, the probability of observing a $j \geq 0$, conditioning $\mathcal{F}_{t-1}$, is

$$Pr(N_t = j|\mathcal{F}_{t-1}) = \frac{e^{-\kappa_t} \kappa_t^j}{j!}, \qquad j = 0, 1, 2, \ldots. \tag{30}$$

Similar to Chan and Maheu (2002), we specify the dynamics of κ_t as

$$\kappa_t = \phi_1 + \phi_2(\kappa_{t-1} - \phi_1) + \phi_3 \xi_{t-1}, \tag{31}$$

where the innovations, ξ_t, are defined as the error in predicting N_t as new information becomes available in $\mathcal{F}_t$. In other words, $\xi_t = E(N_t|\mathcal{F}_t) - E(N_t|\mathcal{F}_{t-1})$, and in terms of model parameters

$$\xi_t = \sum_{j=0}^{\infty} jPr(N_t = j|\mathcal{F}_t) - \kappa_t. \tag{32}$$

The conditions $\phi_1 > 0$ and $1 > \phi_2 > \phi_3 > 0$ are sufficient to ensure positiveness and stationarity of κ_t, see Chan and Maheu (2002). A similar dynamics for the intensity has been adopted by Maheu and McCurdy (2004) and Maheu et al. (2013) for stock returns and by Caporin et al. (2016) for the realized variance. Finally, the filtered probability needed to compute $E(N_t|\mathcal{F}_t)$ is obtained via Bayes' rule, as follows:

$$Pr(N_t = j|\mathcal{F}_t) = \frac{f(\mathcal{A}_t|N_t = j, \mathcal{F}_{t-1})Pr(N_t = j|\mathcal{F}_{t-1})}{f(\mathcal{A}_t|\mathcal{F}_{t-1})}, \tag{33}$$

where the density of $\mathcal{A}_t$ conditional on $N_t = j$ and $\mathcal{F}_{t-1}$ is

$$f(\mathcal{A}_t|N_t = j, \mathcal{F}_{t-1}) = \begin{cases} \frac{1}{\mathcal{A}_t}\left(\frac{\vartheta\mathcal{A}_t}{d_\kappa\mu_t}\right)^{\vartheta} \frac{e^{\left(\frac{-\vartheta\mathcal{A}_t}{d_\kappa\mu_t}\right)}}{\Gamma(\vartheta)}, & N_t = 0 \\ \frac{2}{\mathcal{A}_t}\left(\frac{\mathcal{A}_t}{\mu_t}\frac{\vartheta\zeta}{d_\kappa}\right)\left(\frac{j\zeta+\vartheta}{2}\right)\frac{1}{\Gamma(j\zeta)\Gamma(\vartheta)}\mathbb{K}_{j\zeta-\vartheta}\left(2\sqrt{\frac{\mathcal{A}_t}{\mu_t}\frac{\vartheta\zeta}{d_\kappa}}\right), & N_t = j > 0, \end{cases} \tag{34}$$

where $\mathbb{K}(\cdot)$ is the modified Bessel function of a second kind, while the denominator in (33) is given by the following:

$$f(\mathcal{A}_t|\mathcal{F}_{t-1}) = e^{-\kappa_t} g_{\mathcal{A}_t} + \sum_{j=1}^{\infty} \frac{e^{-\kappa_t}\kappa_t^j}{j!} w_{\mathcal{A}_t}, \tag{35}$$

where $g_{\mathcal{A}_t}$ and $w_{\mathcal{A}_t}$ are $f(\mathcal{A}_t|N_t = j, \mathcal{F}_{t-1}, \alpha, \beta, \gamma)$ for $j = 0$ and $j > 0$, respectively. Therefore, the conditional density of $\mathcal{A}_t$ is a mixture of gamma and kappa distributions, whose weights are governed by the Poisson probabilities and by κ_t. The density is available in closed form, thus allowing us to estimate the model parameters by maximum likelihood. In the following analysis, we distinguish between the AMEM-Mix model with time-varying Poisson intensity (i.e., AMEM-Mix$_{\kappa_t}$) and with constant intensity (i.e., AMEM-Mix$_{\kappa}$), that is, $\kappa_t = \phi_1$.

B.2 Estimation results

Table 9 reports the parameter estimates (and goodness of fit tests) for several AMEM and AMEM-Mix specifications estimated on daily and realized Amihud series of SPY, where the realized Amihud series is computed using returns sampled at 5- and 10-minute frequencies. Panel a) of Table 6 shows the coefficients from the specifications under consideration, which are all estimated using maximum likelihood. As suggested by Engle and Gallo (2006), we allow μ_t to follow asymmetric GARCH-type or asymmetric HAR-type process with asymmetric response to negative returns. Panel b) of Table 6 displays the results of a number of diagnostics tests on the residuals and Poisson intensity innovations, that is, the p-values of the Ljung-Box test (at 1, 5, and 10, lags). Table 10 reports the parameter estimates of the linear and log-linear models. Looking at the estimates of the AMEM models in Table 9, we notice that the parameter α in the volatility literature is generally found in the

range between 0.02 and 0.1 (Bauwens et al., 2012, ch. 1), while we find values in the range between 0.175 and 0.217 for the realized Amihud, signaling that illiquidity is more responsive to news than volatility. Instead, when the AMEM model is estimated on the daily Amihud, the estimates of α are significantly reduced because the daily Amihud is a more noisy proxy of the signal compared with the realized Amihud, so the model assigns a smaller weight to the parameter governing the news. Analogous evidence is found in the volatility literature when employing the realized GARCH model of Hansen et al. (2012) rather than a classic GARCH model on squared returns.

As for the parameter γ, it enters the model with the expected positive sign and is significant across all models, pointing at a more pronounced reaction of illiquidity against negative returns rather than against positive returns. Altogether, by adopting the general view that uncertainty arises when new information reaches the market, we can state that illiquidity is strongly related to uncertainty among investors (as measured by volatility) and that this is responsible for the illiquidity persistence. Conversely, the estimates of the parameter β is around 0.78 across models. This is in the lower bound of the interval of estimates of β typically found for volatility (according to Bauwens et al., 2012, ch. 1, it is usually close to the upper limit of the interval 0.75–0.98). Finally, it is important to emphasize the behavior of the coefficient ϑ in the various AMEM and AMEM-Mix specifications, whose reciprocal is an estimate of the residuals variance. Notably, ϑ increases when moving from the simplest AMEM specifications to the sophisticated AMEM-Mix. Indeed, in the models with the mixtures, a significant part of the variability of the illiquidity is explained by mixture component Z_t. This finding testifies the need for a model that can assign the correct probability to large realizations of the illiquidity measure. As expected, the value of the log-likelihood function is larger for the AMEM-Mix specifications when compared with then simpler AMEM.

As for the Poisson intensity, the process κ_t is very persistent (ϕ_2 is around 0.998), signaling that the number of arrivals strongly depend on its past realizations.

Panel a)	**Estimation results**													
	Daily Amihud		*High–Low Amihud*		*Realized Amihud - 5 minutes*					*Realized Amihud - 10 minutes*				
	$AMEM-HAR$	$AMEM(1,1)$	$AMEM-HAR$	$AMEM(1,1)$	$AMEM-HAR$	$AMEM(1,1)$	$AMEM(2,1)$	$AMEM(2,1)-Mix_k$	$AMEM(2,1)-Mix_{k_t}$	$AMEM-HAR$	$AMEM(1,1)$	$AMEM(2,1)$	$AMEM(2,1)-Mix_k$	$AMEM(2,1)-Mix_{k_t}$
ω	0.0160^a	0.0008^a	0.0052^a	0.0006^a	0.0030^a	0.0008^a	0.0008^a	0.0008^a	0.0008^a	0.0031^a	0.0008^a	0.0009^a	0.0008^a	0.0007^a
	(0.0022)	(0.0003)	(0.0011)	(0.0002)	(0.0007)	(0.0002)	(0.0002)	(0.0002)	(0.0002)	(0.0007)	(0.0002)	(0.0002)	(0.0002)	(0.0002)
α_d	0.0000	0.0176^a	0.0000	0.0759^a	0.1265^a	0.1752^a	0.2070^a	0.1978^a	0.2003^a	0.1252^a	0.1593^a	0.1955^a	0.1851^a	0.1848^a
	(0.0234)	(0.0047)	(0.0227)	(0.0082)	(0.0225)	(0.0193)	(0.0180)	(0.0182)	(0.0181)	(0.0225)	(0.0183)	(0.0166)	(0.0165)	(0.0162)
α_w	0.0011	–	0.3146^a	–	0.3808^a	–	–	–	–	0.3394^a	–	–	–	–
	(0.0494)	–	(0.0476)	–	(0.0401)	–	–	–	–	(0.0417)	–	–	–	–
α_m	0.6595^a	–	0.5549^a	–	0.4087^a	–	–	–	–	0.4432^a	–	–	–	–
	(0.0661)	–	(0.0466)	–	(0.0381)	–	–	–	–	(0.0388)	–	–	–	–
β_1	–	0.9490^a	–	0.8938^a	–	0.7962^a	0.4494^a	0.4287^a	0.4174^a	–	0.8104^a	0.4088^a	0.3958^a	0.3958^a
	–	(0.0100)	–	(0.0107)	–	(0.0219)	(0.0803)	(0.0842)	(0.0847)	–	(0.0213)	(0.0715)	(0.0715)	(0.0709)
β_2	–	–	–	–	–	–	0.3103^a	0.3393^a	0.3501^a	–	–	0.3588^a	0.3820^a	0.3850^a
	–	–	–	–	–	–	(0.0746)	(0.0779)	(0.0784)	–	–	(0.0673)	(0.0673)	(0.0668)
γ	0.0297	0.0406^a	0.0546^a	0.0392^a	0.0399^a	0.0259^a	0.0329^a	0.0352^a	0.0347^a	0.0501^a	0.0299^a	0.0395^a	0.0413^a	0.0408^a
	(0.0235)	(0.0101)	(0.0103)	(0.0053)	(0.0071)	(0.0042)	(0.0051)	(0.0051)	(0.0051)	(0.0072)	(0.0044)	(0.0054)	(0.0053)	(0.0053)
θ	1.4608^a	1.4737^a	12.0371^a	12.1911^a	24.7189^a	24.2300^a	24.4870^a	26.1708^a	27.4063	21.91366^a	21.4118^a	21.6983^a	22.9429^a	24.3646^a
	(0.0361)	(0.0364)	(0.3188)	(0.3146)	(0.5895)	(0.4910)	(0.5108)	(0.7786)	(0.5999)	(0.5023)	(0.5299)	(0.4806)	(0.5672)	(0.5847)
ζ	–	–	–	–	–	–	–	9.2630^a	9.2251^a	–	–	–	7.3968^a	7.7027^a
	–	–	–	–	–	–	–	(1.0397)	(0.6618)	–	–	–	(0.9656)	(0.8691)
ϕ_1	–	–	–	–	–	–	–	0.0242^b	0.0226	–	–	–	0.0186^a	0.0186^b
	–	–	–	–	–	–	–	(0.0109)	(0.0159)	–	–	–	(0.0071)	(0.0085)
ϕ_2	–	–	–	–	–	–	–	–	0.9989^a	–	–	–	–	0.9986^a
	–	–	–	–	–	–	–	–	(0.0006)	–	–	–	–	(0.0008)
ϕ_3	–	–	–	–	–	–	–	–	0.0215^a	–	–	–	–	0.0248^a
	–	–	–	–	–	–	–	–	(0.0046)	–	–	–	–	(0.0072)
LogLik	6465.90	6517.19	9007.54	9080.08	10271.75	10296.32	10308.27	10318.59	10330.85	10114.51	10134.01	10150.41	10159.28	10176.26
LRI	-0.0083	-0.0163	-0.0833	-0.0920	-0.1501	-0.1528	-0.1541	-0.1553	-0.1567	-0.1385	-0.1407	-0.1425	-0.1435	-0.1454
Panel b)	**Ljung-Box statistics (p–value)**													
Residuals: ϵ_t														
LB 1	0.0045	0.0031	0.2788	0.5652	0.6561	0.0007	0.2836	0.2580	0.3039	0.6598	0.0001	0.2147	0.1231	0.1080
LB 5	0.0453	0.0781	0.02132	0.0698	0.1608	0.0034	0.0835	0.0603	0.0599	0.2707	0.0013	0.1114	0.0706	0.0618
LB 10	0.0714	0.0650	0.0980	0.0407	0.0001	0.0000	0.0000	0.0000	0.0000	0.0001	0.0000	0.0000	0.0000	0.0000
Filtered Poisson innovations: ξ_t														
LB 1	–	–	–	–	–	–	–	0.1184	0.0400	–	–	–	0.3115	0.0945
LB 5	–	–	–	–	–	–	–	0.0079	0.0056	–	–	–	0.0070	0.0000
LB 10	–	–	–	–	–	–	–	0.0362	0.0188	–	–	–	0.0678	0.0000

Table 9: AMEM and mixture–AMEM estimated coefficients with robust standard errors (White, 1980) and p-value of the Ljung-Box statistics. Superscript *a, b* and *c* denote the 1%, 5%, and 10% significance levels, respectively. For the AMEM–Mix specification, we consider the model with constant jump intensity ($AMEM-Mix_K$, i.e., $\phi_2 = \phi_3 = 0$) and with dynamic jump intensity ($AMEM-Mix_{K_t}$). Sample period: January 3, 2006 – June 29, 2018.

B.3 Linear specifications

We also consider linear specifications based on the HAR model of Corsi (2009). In particular, the linear asymmetric HAR (linear AHAR) model is given by

$$\mathcal{A}_t = \omega + \alpha_d \mathcal{A}_{t-1} + \alpha_w \bar{\mathcal{A}}_{w,t-1} + \alpha_m \bar{\mathcal{A}}_{m,t-1} + \gamma D_{t-1} \mathcal{A}_{t-1} + \varepsilon_t, \tag{36}$$

and the log-linear AHAR (log-linear AHAR) specification given by

$$\log \mathcal{A}_t = \omega + \alpha_d \log \mathcal{A}_{t-1} + \alpha_w \log \bar{\mathcal{A}}_{w,t-1} + \alpha_m \log \bar{\mathcal{A}}_{m,t-1} + \gamma D_{t-1} \log \mathcal{A}_{t-1} + \varepsilon_t, \tag{37}$$

Panel a)	**Estimation results**					
	Daily Amihud		*High–Low Amihud*		*Realized Amihud*	
	Loglinear AHAR	Linear AHAR	Loglinear AHAR	Linear AHAR	Loglinear AHAR	Linear AHAR
ω	-1.6182^a	0.0148^a	-0.3237^a	0.0057^a	-0.2024^a	0.0027^a
	(0.2231)	(0.0025)	(0.0663)	(0.0015)	(0.0439)	(0.0006)
α_d	-0.0275	-0.0838^a	0.0304	-0.0152	0.1448^a	0.1171^a
	(0.0227)	(0.0283)	(0.0207)	(0.0223)	(0.0259)	(0.0261)
α_w	0.0406	0.0556	0.3313^a	0.3534^a	0.3711^a	$0.4208^a$$
	(0.0542)	(0.0575)	(0.0526)	(0.0576)	(0.0568)	(0.0730)
α_m	0.5244^a	0.7017^a	0.5428^a	0.5190^a	0.4253^a	0.3872^a
	(0.0845)	(0.0832)	(0.0496)	(0.0570)	(0.0513)	(0.0633)
γ	-0.0259^a	0.0561^b	-0.0210^a	0.0565^a	-0.0135^a	0.0366^a
	(0.0100)	(0.0214)	(0.0032)	(0.0107)	(0.0024)	(0.0067)
Panel b)	**Ljung-Box statistics (p–value)**					
LB(1)	0.9764	0.9260	0.5730	0.5507	0.5923	0.7050
LB(5)	0.8462	0.6273	0.2495	0.7036	0.0827	0.1768
LB(10)	0.4676	0.3781	0.0970	0.2749	0.0000	0.0000

Table 10: AHAR estimated coefficients with robust standard errors (White, 1980) and p-value of the Ljung-Box statistics. Superscript *a, b* and *c* denote the 1%, 5%, and 10% significance levels, respectively. Sample period: January 3, 2006 – June 29, 2018.

B.3.1 PITs

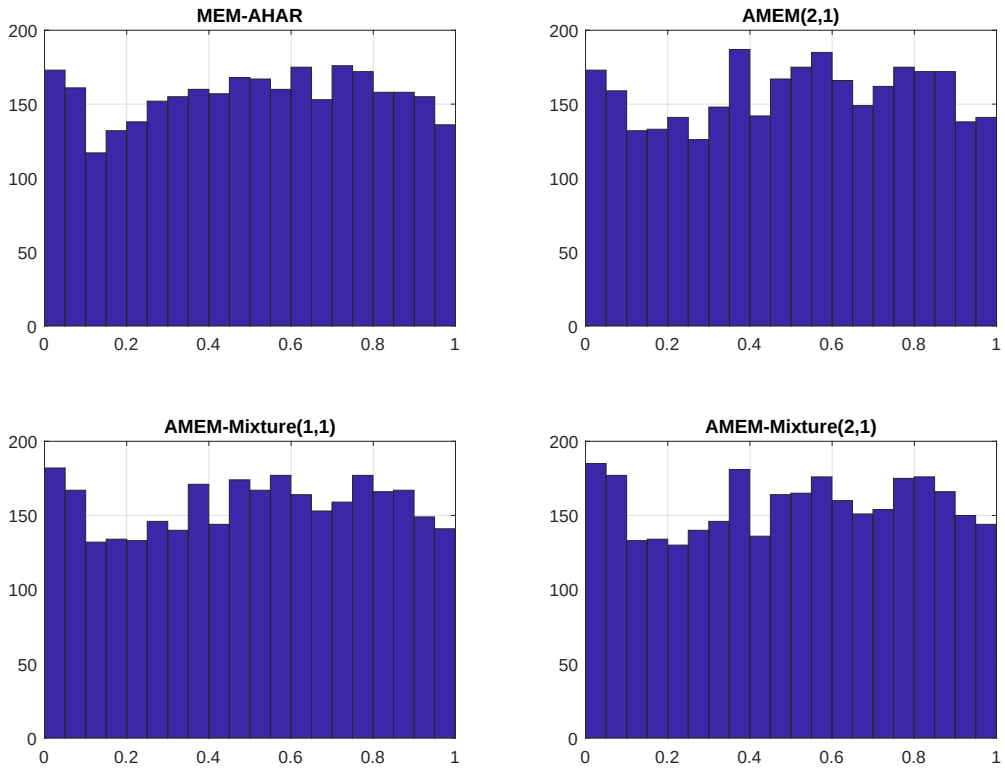

Figure 9: Probability integral transform (PIT) from MEM-HAR, AMEM(2,1) and mixture–AMEM . Sample period: January 3, 2006 – June 29, 2018.

B.4 The USD/CHF analysis

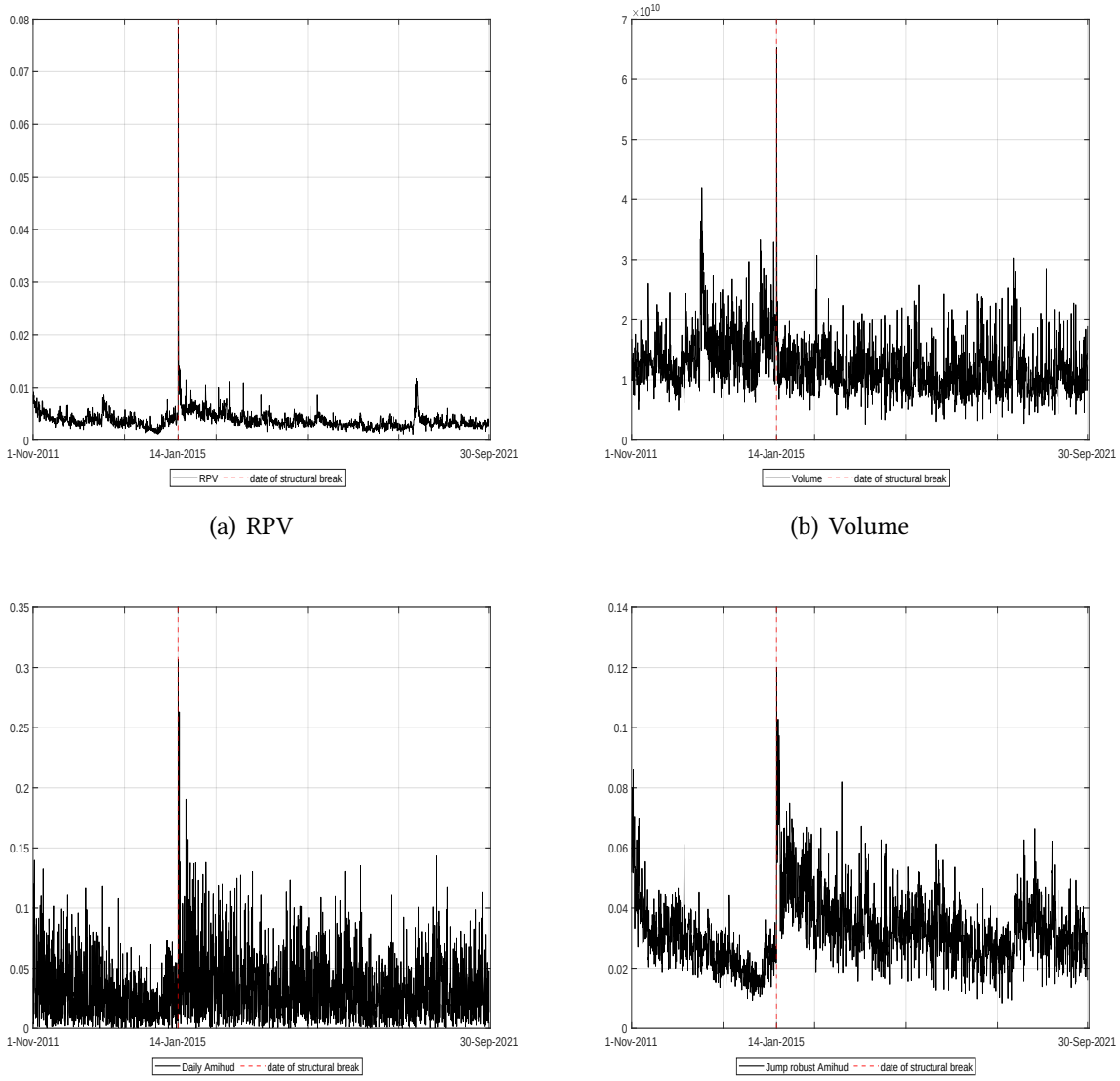

(a) RPV

(b) Volume

(c) Daily Amihud

(d) Realized Amihud

Figure 10: Break dates. The figures report the time series of RPV, volume, daily Amihud, and realized Amihud for the USD/CHF rate (black solid line). The red vertical line denotes the break date, which is estimated by means of the Bai and Perron (1998) test for unknown break points. The test is performed with 15% trimming at the beginning and the end of the sample period and between break dates.